N-REPRESENTABLE ONE ELECTRON DENSITIES CALCULATED FROM X-RAY STRUCTURE FACTORS

by

Patricia Oldfield

A dissertation submitted to the Graduate Faculty in Chemistry in partial fulfillment of the requirements for the degree of Doctor of Philosophy, The City University of New York.

1975

This manuscript has been read and accepted for the Graduate Faculty in Chemistry in satisfaction of the dissertation requirement for the degree of Doctor of Philosophy.

8.1.75
date

Chairman of Examining Committee

8/5/75
date

Executive Officer

Supervisory Committee

The City University of New York

Abstract

N-Representable One Electron Densities
calculated from X-Ray Structure Factors
by
Patricia Oldfield
Adviser: - Dr. Louis Massa

A least squares method was used to obtain the matrix representative $\underset{\sim}{P}$ of the one electron density, from theoretical X-Ray structure factors calculated for model one electron systems. In one case the matrix $\underset{\sim}{P}$ was constrained to be idempotent, ensuring N-Representability in the Hartree-Fock Approximation. In the other case this constraint was omitted. It was found that neglecting the idempotency constraint could result in negative densities and a violation of the variational principle. The calculation of expectation values showed that although the unconstrained $\underset{\sim}{P}$ matrix always fit the structure factor data better, it did not necessarily predict the most accurate expectation value. Some of the eigenvalues obtained by diagonalizing published $\underset{\sim}{P}$ matrices, resulting from a least squares method without the idempotency constraint, were shown to be quantum mechanically invalid.

Acknowledgements

I heartily thank Dr. Louis Massa for his guidance and many interesting and helpful discussions. I thank Dr. Carol Frishberg and Dr. Gary Schnuelle for their discussions on certain aspects of this work. To those who have sought to keep me aware of the more fundamental Laws of Nature, during the course of this thesis, I am deeply in debt.

Contents

List of Tables

List of Figures

Chapter I

X-Ray Diffraction is a technique which has historically been used for determining relative atomic positions and therefore bond lengths and bond angles between atoms in the unit cell of a crystal. The relationship between the intensity of scattered X-rays and the electron density is given by

$$F(\vec{K})\,F(\vec{K})^{*} = I(\vec{K}) \qquad \text{(I-1)}$$

$$F(\vec{K}) = \int \rho(\vec{r})\, e^{2\pi i \vec{K}\cdot\vec{r}}\, d^{3}\vec{r} \qquad \text{(I-2)}$$

where $\vec{K}$ is the vector bisecting the incoming and scattered X-ray beams, of magnitude $2\sin\theta/\lambda$

$F(\vec{K})$ is the scattering amplitude

$I(\vec{K})$ is the intensity of the diffracted X-Rays

$F(\vec{K})$ is thus the fourier transform of the electron density and for an asymmetric density is a complex quantity. The scattered wave in any direction is clearly the sum of the waves scattered from all positions $\vec{r}$ of electron density. In order to reconstruct the density we need to know the structure factor, $F(\vec{K})$, but only the magnitude, $|F|$, is obtainable from the experimental X-ray results. The crystallographic method consists of devising a trial structure, using an approximate model to construct $F(\vec{K})$ and finally refining the model by comparison of the absolute magnitudes of the calculated structure factors with those obtained from experiment.

Until recently the model assumed scattering from independent spherical densities located at the atomic positions. The atomic scattering power of an atom was given by

$$f_n(|\vec{K}|) = \int \rho_n(|\vec{r}|)\, e^{2\pi i |\vec{K}||\vec{r}|}\, d^3\vec{r} \qquad \text{(I-3)}$$

where the density $\rho(|\vec{r}|)$ is spherically symmetrical. f_n is the amplitude of the wave scattered from atom n, relative to the wave scattered from the origin in the same direction. To obtain the total wave in direction $\vec{K}$, it is only necessary to sum the waves from each atom with the appropriate phase. If $\vec{r}_n$ is the distance from an arbitrary origin to atom n, the expression is simply

$$F(\vec{K}) = \sum_n f_n\, e^{2\pi i \vec{K}\cdot\vec{r}_n} \qquad \text{(I-4)}$$

When $\vec{r}_n$ is expressed in fractions of the unit cell dimensions and the Laue conditions imposed, the expression becomes

$$F(h,k,l) = \sum_n f_n\, e^{2\pi i (hx_n + ky_n + lz_n)} \qquad \text{(I-5)}$$

For every direction given by h, k, 1 the real and imaginary parts of F(h, k, 1) define the amplitude and phase of the calculated structure factor.

Adjustments in atomic positions, in order to obtain the best possible representation of the experimental data, are made by refinement procedures. Fourier synthesis involves computing the density from the observed scattering amplitudes and the calculated phases and subtracting from it the density assumed by the model. This gives rise to a difference map.

Atomic positions, i.e. positions of maximum density, are then adjusted to minimize the contours in the difference map. The least squares refinement, more commonly used nowadays, minimizes the functional

$$\mathcal{H} = \sum_{\vec{k}} \omega_{\vec{k}} \left[F_o(\vec{k}) - s|F_c(\vec{k})| \right]^2 \qquad (I\text{-}6)$$

where $\omega_{\vec{k}}$ is the weighting factor,

F_o is the observed structure factor and

$$F_c(h,k,l) = \sum_n f_n e^{2\pi i(hx_n + ky_n + lz_n)} \cdot T_n \qquad (I\text{-}7)$$

with respect to the positional parameters, thermal parameters as defined in T_n and the scale factor s. This method requires that there be many more observations than parameters and that the equations are linear in the parameters. If a good trial structure is known a linear set of equations can be obtained by minimizing $\mathcal{H}$ with respect to the shift in parameters, relative to the trial parameters. An indication of a good structure is the value of the R factor

$$\text{i.e.} \quad R = \left\{ \sum_{\vec{k}} \omega_{\vec{k}} \left[F_o(\vec{k}) - s|F_c(\vec{k})| \right]^2 \Big/ \sum_{\vec{k}} \omega_{\vec{k}} F_o^2(\vec{k}) \right\}^{1/2} \qquad (I\text{-}8)$$

R factors of the order 0.04 are at present reported with good diffraction data.[1]

Unfortunately the outline given above is grossly oversimplified. Firstly, the scattering amplitude F_o is obtainable only after the intensity has been corrected for absorption, extinction and geometric effects. At this stage it still contains a scale factor and is related to the thermally

perturbed, rather than the static density obtained from theoretical calculations. As indicated previously, these effects are accounted for by parametrization in the least squares refinement. However, since a sum of spherical atomic densities is being used to fit a molecular density, it is conceivable that the temperature factors are adjusted in the least squares fit to simulate the valence and lone pair densities which arise during molecular formation. That this is indeed the case has been shown by Coppens[2] in his comparison of thermal parameters from X-ray and neutron diffraction. Since for a molecule with a closed shell structure the scattering of neutrons is due to the nuclei alone, the point charge approximation for the scattering material gives more reliable temperature factors and atomic positions. Atomic positions from X-ray data may also be in error due to the shift in the centroids of electron density when the atoms form a molecule. The shortening of the internuclear distance between hydrogen and other atoms, of magnitude ~ 0.1Å, compared to the bond distances obtained from neutron data is a well known phenomenon.[3] The discrepancy in internuclear distances calculated from X-Ray and Neutron Diffraction data is of the order 0.01 - 0.02Å for first row atoms.[4] Thus atomic and thermal parameters obtained from conventional treatment of X-Ray data may be in error, even though the R value and Difference Fourier Synthesis indicate a correct structure. It must be noted that it is only in recent years, due to the improvement of X-Ray Diffraction techniques, that the finer details of

the molecular electron density and hence the above errors have been detected.

Several ways to reduce these errors have been suggested. As previously indicated, position and thermal parameters obtained from neutron diffraction are more reliable. A disadvantage of this approach is that an additional experiment and larger crystal are required. A comparison of the data from both experiments also requires a thorough analysis of errors in order to be meaningful.[5] Scale factors are most reliably determined experimentally.[6] High angle refinement of X-Ray data is thought to give more reliable parameters, than a fit to the full range of structure factors.[7] This is due to the nature of the fourier transform. The more diffuse densities associated with the atomic valence orbitals become the more contracted fourier transforms, (see for example Figure I) as compared with the core electron transforms and are therefore expected to contribute much less to the scattering amplitudes at higher scattering angles. However there are some discrepencies between high angle and neutron diffraction analyses. It is now thought that the contribution to the scattering amplitude from lone pair densities is considerable at higher angles and this may account for such differences.[9] The Double Atom[10] and Sharpened Atom[11] Refinements attempt to minimize the errors inherent in the model, by allowing additional positional and occupancy parameters for the valence shell density and giving higher weights to higher angle scattering, respectively.

However, the real problem lies in the nature of the model used. The sum of spherical densities alone cannot accurately represent a molecular density. It is, in essence, the errors in the thermal and positional parameters which allow the molecular density to be well represented by this model. This allows some understanding of the redistribution of electron density during molecular formation, through the concept of difference density maps.[2] The density assumed by the model when calculated with accurate positional and thermal parameters from neutron diffraction data, is subtracted from the density obtained by conventional X-ray analysis. Negative and positive density contours thus indicate removal and build up respectively of density in the molecule as compared to the isolated atoms. Coppens recommends that atomic scattering factors for use in difference density maps be calculated from Hartree Fock atomic wavefunctions.[12] Stewart has suggested using the fourier transforms of only core electrons in order to obtain a valence difference map.[13]

Clearly to obtain accurate charge densities from X-Ray Diffraction data for comparison with theoretical calculations, it is desirable to account for the redistribution of electrons during molecular formation in the initial model itself. Atomic asphericity has been accounted for by the suitable choice of wave functions centered at each atomic position.[14] In the L-Shell (LS)[15] and Extended L Shell(ELS)[6] treatments the atomic scattering factor is partitioned into a contribution from the core and valence scattering terms. The occupancy of

the valence orbitals, P, is a parameter to be determined in the conventional least squares refinement (ELS) or in a separate cycle after the conventional refinement (LS). Although these methods are an improvement over the use of the conventional Hartree Fock atomic scattering factor, they do not explicitly account for the scattering from the "bond density" between atoms. The inclusion of such bond scattering terms was first suggested by McWeeney[16] and later generalized by Stewart.[17] In the Hartree Fock approximation, the one electron density is simply the sum of the density contributions from each occupied orthogonal molecular orbital. Introducing the LCAO approximation, the density can then be expressed in terms of basis functions $\{\psi_i\}$ and population coefficients, $P_{\mu\nu}$

i.e.

$$\rho(1,1') = 2 \sum_n \phi_n(1)\, \phi_n^*(1')$$

$$\phi_n = \sum_\mu c_{\mu n}\, \psi_\mu$$

thus
$$\rho(1,1') = 2 \sum_n \sum_\mu \sum_\nu c_{\mu n} c_{\nu n}\, \psi_\mu(1)\, \psi_\nu^*(1')$$

$$= 2 \sum_\mu \sum_\nu P_{\mu\nu}\, \psi_\mu(1)\, \psi_\nu^*(1') \qquad \text{(I-9)}$$

thus
$$F(\vec{k}) = \int \rho(1,1')\, e^{2\pi i \vec{k}\cdot\vec{r}}\, d^3\vec{r}$$

$$= 2 \sum_\mu \sum_\nu P_{\mu\nu} \int \psi_\mu(1)\, e^{2\pi i \vec{k}\cdot\vec{r}}\, \psi_\nu(1')\, d^3\vec{r}$$

$$= 2 \sum_{\mu,\nu} P_{\mu\nu}\, f_{\mu\nu}(\vec{k}) \qquad \text{(I-10)}$$

Stewart has given analytical expressions for calculating one and two center terms using gaussian expansions of HF or STO basis functions.[17,18,19] If accurate positional and thermal parameters have already been determined, this formalism can be used in order to obtain the population parameters from a least squares refinement in which

$$F_c(\vec{K}) = \sum_{\mu,\nu} P_{\mu\nu} f_{\mu\nu}(\vec{K}) \qquad T(\phi_\mu \phi_\nu)$$

and the functional to be minimized is as usual,

$$H = \sum_{\vec{K}} w_{\vec{K}} \left[F_o(\vec{K}) - s F_c(\vec{K}) \right]^2$$

Coppens and coauthors have developed and used this method to study several small and medium sized molecules[20,6,21,22]. Two models have been used. In the one center model all fourier transforms of orbital products centered on different atoms are neglected. In the two center model such terms are included and only products between non-bonded atoms are neglected. It is the two center model which specifically accounts for scattering from bond density. The number of parameters are reduced, in order to make the least squares method meaningful, by molecular and bond symmetry considerations. The bond temperature factors between atoms A and B are taken as

$$T_{ab} = (T_a + T_b)/2$$

Due to the large correlation of parameters and comparison with accurate theoretical calculations on diborane,[22] it has been concluded that the net atomic charges on atoms are more accurately determined than individual population parameters. Comparison of results from the one center model with INDO

atomic charges show reasonable qualitative agreement when molecule optimized Slater type minimal basis functions are used for cyanuric acid and α-oxalic acid dihydrate.[6] However, using the two center model for cyanuric acid,[22] the isolated atom Hartree Fock basis functions are found to give the lower R value, which corresponds to the most reasonable basis set as judged by the diborane calculations. The atomic and bond charges for TCEO[21] do not in general give results expected from theory, nor do they agree with the ELS calculations performed on the same molecule. The authors note that the physically unreasonable negative bond densities are probably due to correlation between the bond and one center parameters. However the population asphericity map[6] from the two center calculation agrees qualitatively with the X-N difference density map. Comparison of theoretical difference density maps from INDO and ab initio STO-3G calculations with the best population asphericity map from the theoretical studies of diborane, indicate that the approximate theoretical calculations do not place enough density in the bonding or lone pair regions. Jones et al have recommended transforming the population parameters to a set of uncorrelated parameters[22] to allow meaningful comparison with theoretical population parameters.

It is the attainment of just such meaningful comparisons which provides the motivation for the present study. Even with the determination of uncorrelated parameters, such comparisons are not theoretically valid. In order to be quan-

tum mechanically correct the one electron density must be N-Representable. It is easily shown that the necessary and sufficient condition for single determinant N-Representability is the idempotency of the P matrix, the latter being defined in equation (I-9) (see Chapter II).

In the following study various theoretical model densities have been fit in a least squares procedure analagous to that used by Coppens and several authors[6,20,21,22] and via the method developed by Clinton et al[23,24,25], which imposes the idempotency constraint. Comparison of densities, eigenvalues and expectation values from the two methods, with those of the model density have been made. Expectation values may be considered criteria for judging a good density distribution.[26] This study shows that the density which gives the best fit to the data, via the unconstrained least squares method, does not necessarily predict the most accurate expectation values. In some cases the omission of the idempotency constraints leads to negative densities and energy expectation values which violate the variational principle. Diagonalization of the published $\underset{\sim}{P}$ matrices for TCEO[21] show that some of the eigenvalues of the one electron density fall outside the quantum mechanically valid range.

Chapter II

Theoretically the one electron density is related to the wave function of the system through

$$\rho(1,1') = N \int \psi(1,2\ldots N)\, \psi^*(1',2\ldots N)\, d\tau_2 \ldots d\tau_N$$

and describes the probability of finding an electron at any position in space. The problem of relating the one electron function to an N electron function, through the above equation, is the N-Representability Problem. As shown in Chapter I, (I-9), when the wave function is approximated as a single determinant, the one electron density may be expressed in terms of the basis functions $\{\psi_i\}$ and the matrix representation $\underset{\sim}{P}$

i.e. $$\rho(1,1') = \mathrm{Tr}\ \underset{\sim}{P}\ \underset{\sim}{\psi}(1)\, \underset{\sim}{\psi}^*(1')$$

In this case the necessary and sufficient conditions for N-Representability are that $\underset{\sim}{P}$ be idempotent ($\underset{\sim}{P} = \underset{\sim}{P}^2$) hermitian ($\underset{\sim}{P} = \underset{\sim}{P}^{+}$) and normalized to the number of electrons in the system ($\mathrm{Tr}\ \underset{\sim}{P} = N$).

The necessity of these conditions can be seen as follows:

In the Hartree-Fock Approximation

$$\psi(1\ldots N) = 1/\sqrt{N!} \sum_n \phi_n(1)\, \chi_n(2\ldots N)$$

where $\chi_n(2\ldots N)$ is the cofactor of ϕ_n, a molecular orbital in the Slater determinant.

Thus

$$N \int \psi(1\ldots N)\, \psi^*(1\ldots N)\, d\tau_2 \ldots d\tau_N$$

$$= N/N! \sum_{n,m} \phi_n(1)\, \phi_m^*(1) \int \chi_n(2\ldots N)\, \chi_m^*(2\ldots N)\, d\tau_2 \ldots d\tau_N$$

The ϕ's may be taken as orthonormal and thus

$$\langle \chi_m | \chi_n \rangle = (N-1)!\, \delta_{mn}$$

so that the one electron density becomes

$$\rho(1,1') = \sum_n \phi_n(1)\, \phi_n^*(1') = \mathrm{Tr}\, \underset{\sim}{\phi}(1)\, \underset{\sim}{\phi}^{+}(1')$$

where $\underset{\sim}{\phi}$ is a column matrix of molecular orbitals. If we choose a basis set $\{\psi_i\}$ to represent each molecular orbital ϕ, then

$$\underset{\sim}{\phi} = \underset{\sim}{C}\, \underset{\sim}{\psi}$$

and
$$\rho(1,1') = \mathrm{Tr}\, \underset{\sim}{C}\, \underset{\sim}{\psi}(1)\, \underset{\sim}{\psi}^{+}(1')\, \underset{\sim}{C}^{+}$$

$$= \mathrm{Tr}\, \underset{\sim}{C}^{+}\underset{\sim}{C}\, \underset{\sim}{\psi}(1)\, \underset{\sim}{\psi}^{+}(1')$$

$$= \mathrm{Tr}\, \underset{\sim}{P}\, \underset{\sim}{\psi}(1)\, \underset{\sim}{\psi}^{+}(1')$$

From the orthonormality of the molecular orbitals

$$\underset{\sim}{\phi} \cdot \underset{\sim}{\phi}^{+} = \underset{\sim}{1} \quad \text{so} \quad \underset{\sim}{C}\underset{\sim}{\psi} \cdot \underset{\sim}{\psi}^{+}\underset{\sim}{C}^{+} = \underset{\sim}{1}$$

$$\text{or} \quad \underset{\sim}{C}\, \underset{\sim}{S}\, \underset{\sim}{C}^{+} = \underset{\sim}{1}$$

In the case of an orthonormal basis set this implies

$$\underset{\sim}{C}\underset{\sim}{C}^{+} = \underset{\sim}{1} \qquad \underset{\sim}{C}^{+}\underset{\sim}{C}\underset{\sim}{C}^{+}\underset{\sim}{C} = \underset{\sim}{C}^{+}\underset{\sim}{C}$$

Thus the definition of $\underset{\sim}{P} = \underset{\sim}{C}^{+}\underset{\sim}{C}$ in an orthonormal basis set implies that $\underset{\sim}{P}$ is an idempotent matrix. The necessity that $\underset{\sim}{P}$ be hermitian and normalized follows simply from

$$(\underset{\sim}{C}^{+}\underset{\sim}{C})^{+} = \underset{\sim}{C}^{+}\underset{\sim}{C}$$

and

$$\int \rho(1,1')\, d\tau_1 = N = \mathrm{Tr}\, \underset{\sim}{P}\, \underset{\sim}{S} = \mathrm{Tr}\, \underset{\sim}{P} \quad \text{for } \underset{\sim}{S} = \underset{\sim}{1}$$

That these conditions are sufficient to ensure N-Representability can be seen from a theorem due to McWeeny.[27]

i.e. Assume $\underset{\sim}{P} = \underset{\sim}{P}^2$, $\underset{\sim}{P} = \underset{\sim}{P}^+$ and $\mathrm{Tr}\ \underset{\sim}{P} = N$.

Then, since any hermitian matrix can be diagonalized by a unitary transformation

$$\underset{\sim}{U}\ \underset{\sim}{P}\ \underset{\sim}{U}^+ = \bar{\underset{\sim}{P}}$$

and $$(\underset{\sim}{U}\ \underset{\sim}{P}\ \underset{\sim}{U}^+)(\underset{\sim}{U}\ \underset{\sim}{P}\ \underset{\sim}{U}^+) = \bar{\underset{\sim}{P}}^2$$

but since $\underset{\sim}{U}^+\underset{\sim}{U} = 1$ and $\underset{\sim}{P}^2 = \underset{\sim}{P}$ then $\bar{\underset{\sim}{P}}^2 = \bar{\underset{\sim}{P}}$

Thus $\bar{\underset{\sim}{P}}$ must be a diagonal matrix with diagonal elements of only 1 or 0. Due to the normalization constraint and the invariance of the trace to a unitary transformation

$$\text{i.e.}\quad \mathrm{Tr}\ \underset{\sim}{P} = \mathrm{Tr}\ \underset{\sim}{U}\ \underset{\sim}{P}\ \underset{\sim}{U}^+ = N$$

there must be N diagonal elements of magnitude 1. Examination of the reverse transformation

$$\underset{\sim}{P} = \underset{\sim}{U}^+\ \bar{\underset{\sim}{P}}\ \underset{\sim}{U} = \underset{\sim}{U}^+\begin{pmatrix} 1_N & \\ & 0 \end{pmatrix}\underset{\sim}{U} = \underbrace{\underset{\sim}{U}^+\begin{pmatrix} 1_N & \\ & 0 \end{pmatrix}}_{\widehat{\underset{\sim}{1}}^+}\underbrace{\begin{pmatrix} 1_N & \\ & 0 \end{pmatrix}\underset{\sim}{U}}_{\widehat{\underset{\sim}{1}}}$$

shows that $\underset{\sim}{P}$ may be factorized into the product of a matrix $\widehat{\underset{\sim}{1}}$ with its adjoint, where $\widehat{\underset{\sim}{1}}$ contains the first N rows of the matrix $\underset{\sim}{U}$. Thus we see that any hermitian, idempotent and normalized matrix $\underset{\sim}{P}$ used in the one electron density expression,

$$\text{i.e.}\quad \mathrm{Tr}\ \underset{\sim}{P}\ \underset{\sim}{\psi}(1)\ \underset{\sim}{\psi}^+(1')$$

is sufficient to ensure N-Representability, in the case of an N-electron single determinant wave function, due to the

factorization

$$\underset{\sim}{P} = \underset{\sim}{T}^{+}\underset{\sim}{T}$$

and thus $\rho(1,1') = Tr\, \underset{\sim}{T}^{+}\underset{\sim}{T}\,\underset{\sim}{\Psi}(1)\underset{\sim}{\Psi}^{+}(1') = Tr\, \underset{\sim}{T}\,\underset{\sim}{\Psi}(1)\underset{\sim}{\Psi}^{+}(1')\underset{\sim}{T}^{+}$

$$= Tr\, \underset{\sim}{\Phi}(1)\,\underset{\sim}{\Phi}^{+}(1')$$

where $\underset{\sim}{\Phi} = \underset{\sim}{T}\,\underset{\sim}{\Psi}$

and $\underset{\sim}{\Phi}$ may be taken as the N orbitals in the single determinant N electron wave function.

In the method of Clinton et al a set of iterative equations have been developed[28] which generate an idempotent matrix $\underset{\sim}{P}$ and satisfy the constraints

$$Tr\ \underset{\sim}{P} = N$$

$$Tr\ \underset{\sim}{P}\ \underset{\sim}{f}(\vec{K}) = F(\vec{K}), \quad \text{for all } \vec{K} \text{ measured.}$$

When $F(\vec{K})$ are taken as the crystallographic structure factors, the elements of $\underset{\sim}{f}(\vec{K})$ are given by

$$f_{ij}(\vec{K}) = \int \psi_i\, e^{2\pi i \vec{K}\cdot\vec{r}}\, \psi_j\, d^3\vec{r}$$

The idempotency of $\underset{\sim}{P}$ is ensured by minimizing the quantity $Tr\ (\underset{\sim}{P} - \underset{\sim}{P}^2)^2$. In practice the normalization constraint is included, as the zeroth equation, with the experimental constraints. Thus the two constraints

$$Tr\ (\underset{\sim}{P} - \underset{\sim}{P}^2)^2 = 0$$

$$Tr\ \underset{\sim}{P}\ \underset{\sim}{f}(\vec{K}) = F(\vec{K})$$

can be satisfied simultaneously using Lagrange's method by

which

$$\mu(P,\lambda) = Tr\,(\underset{\sim}{P}-\underset{\sim}{P}^2)^2 + \sum_{\vec{K}} \lambda_{\vec{K}} \left\{ Tr\,\underset{\sim}{P}\,\underset{\sim}{f}(\vec{K}) - F(\vec{K}) \right\}$$

is minimized with respect to $\underset{\sim}{P}$ and λ_k. Minimizing with respect to λ, returns the experimental constraints

$$Tr\ \underset{\sim}{P}\ \underset{\sim}{f}(\vec{K}) = F(\vec{K})$$

Minimizing with respect to $\underset{\sim}{P}$ gives

$$\delta \left\{ Tr\,(\underset{\sim}{P}^2+\underset{\sim}{P}^4-2\underset{\sim}{P}^3) + \sum_{\vec{K}} \lambda_{\vec{K}} \left(Tr\,\underset{\sim}{P}\,\underset{\sim}{f}(\vec{K}) - F(\vec{K}) \right) \right\} = 0$$

$$\text{i.e. } Tr\left[2\underset{\sim}{P}+4\underset{\sim}{P}^3-6\underset{\sim}{P}^2\right]\delta P + \sum_{\vec{K}} \lambda_{\vec{K}}\, Tr\,\underset{\sim}{f}(\vec{K})\,\delta\underset{\sim}{P} = 0$$

$$\text{or } Tr\left\{ \underset{\sim}{P} + 2\underset{\sim}{P}^3 - 3\underset{\sim}{P}^2 - \sum_{\vec{K}} \lambda'_{\vec{K}}\, \underset{\sim}{f}(\vec{K}) \right\} \delta\underset{\sim}{P} = 0$$

In order for the trace of the product matrices to be zero for arbitary $\delta\underset{\sim}{P}$

$$\underset{\sim}{P} + 2\underset{\sim}{P}^3 - 3\underset{\sim}{P}^2 - \sum_{\vec{K}} \lambda'_{\vec{K}}\, \underset{\sim}{f}(\vec{K}) = 0$$

must hold. Rearranging we obtain

$$\underset{\sim}{P}_{n+1} = 3\underset{\sim}{P}_n^2 - 2\underset{\sim}{P}_n^3 + \sum_{\vec{K}} \lambda'_{\vec{K}}\, \underset{\sim}{f}(\vec{K})$$

The method involves a first guess at $\underset{\sim}{P}_n$ which is substituted into

$$Tr\ \underset{\sim}{P}_{n+1}\ \underset{\sim}{f}(\vec{K}) = F(\vec{K})$$

which reduces to a matrix equation

$$\underset{\sim}{\lambda}^n = \underset{\sim}{T}^{-1}\ \underset{\sim}{\Delta}^{(n)}$$ [28]

the solutions of which give the λ's. These values are returned to the iterative equation and the process repeated

until an idempotent $\underset{\sim}{P}$ matrix is reached. If there are more experimental values, $F(\vec{K})$, than parameters to be determined, the set of K equations, $T_r \underset{\sim}{P} \underset{\sim}{f}(\vec{K}) = F(\vec{K})$, give no consistent solution. The most accurate fit to all F(K) is given by minimizing the quantity

$$TF = \sum_{\vec{K}} \omega_{\vec{K}} \left[F(\vec{K}) - Tr \underset{\sim}{P} \underset{\sim}{f}(\vec{K}) \right]^2$$

or using the constraint

$$\sum_{\vec{K}} \omega_{\vec{K}} \left(F(\vec{K}) - Tr \underset{\sim}{P} \underset{\sim}{f}(\vec{K}) \right)^2 = \varepsilon$$

where ε is a minimum. Using this equation as a constraint generates a complicated set of iterative equations. A simpler set of equations can be found using the similar constraint

$$\varepsilon = \sum_{\vec{K}} \omega_{\vec{K}} \left| F(\vec{K}) - Tr \underset{\sim}{P} \underset{\sim}{f}(\vec{K}) \right|$$

These are of the form[25]

$$\underset{\sim}{P}_{n+1} = 3\underset{\sim}{P}_n^2 - 2\underset{\sim}{P}_n^3 + \lambda'_{\vec{K}} \left\{ \sum_{\vec{K}\pm} \omega_{\vec{K}\pm} \underset{\sim}{f}(\vec{K}\pm) \right\} + \lambda_N \underset{\sim}{1}$$

where $\underset{\sim}{f}(\vec{K})\pm$ refer to $\underset{\sim}{f}$ matrices for $|F - T_r \underset{\sim}{P} \underset{\sim}{f}|$ positive or negative. These values have to be determined at each iteration and ε is minimized in a superiterative procedure.

The method being used at present by many workers in this field in its simplest form minimizes the functional

$$TF = \sum_{\vec{K}} \omega_{\vec{K}} \left[F(\vec{K}) - Tr \underset{\sim}{P} \underset{\sim}{f}(\vec{K}) \right]^2$$

with respect to the elements of $\underset{\sim}{P}$. The number of parameters therefore contained in the hermitian matrix $\underset{\sim}{P}$, normalized to the number of electrons N, in the system is

$$p_N(m) = \frac{m(m+1)}{2} - 1$$

where m is the number of basis functions used. It should be noted that constraining $\underset{\sim}{P}$ to be idempotent reduces the number of parameters to

$$P_I\ (m,\ N) = N(m - N)$$

since there are m x N parameters in the $\underset{\sim}{c}$ matrix defining $\underset{\sim}{P} = \underset{\sim}{c}^{+}\underset{\sim}{c}$, which are reduced due to the N^2 orthogonalization and normalization constraints contained in $\underset{\sim}{c}\ \underset{\sim}{c}^{+} = 1$. For example, when N = 1 and m = 2, as in this study, the number of parameters in the idempotent and non-idempotent matrices are 1 and 2 respectively. Thus an idempotent matrix representative of the density not only ensures N-Representability but should also allow the use of a larger basis set than the non-idempotent representative while maintaining the same amount of overdetermination. Omitting the idempotency constraint, however, always allows a better fit to the data due to the larger number of parameters.

For the case of a one electron system, an identically idempotent, normalized $\underset{\sim}{P}$ matrix may be generated by choosing elements such that

$$\sum_i P_{ii} = 1$$

and

$$P_{ij} = P_{ii}^{1/2} P_{jj}^{1/2}$$

thus

$$P_{ij}^2 = \sum_k P_{ii}^{1/2} P_{kk}^{1/2} P_{kk}^{1/2} P_{jj}^{1/2}$$

$$= P_{ii}^{1/2} P_{jj}^{1/2} \sum_k P_{kk}$$

$$= P_{ii}^{1/2} P_{jj}^{1/2} = P_{ij}$$

In a two dimensional basis, the idempotent matrix $\underset{\sim}{P}_I$ thus takes the form

$$\begin{pmatrix} P & \pm P^{1/2}(1-P^{1/2}) \\ \pm P^{1/2}(1-P)^{1/2} & 1-P \end{pmatrix}$$

It is also noted that since every hermitian matrix can be diagonalized by a unitary transformation

$$\rho(1,1') = \mathrm{Tr}\ \underset{\sim}{U}\,\underset{\sim}{P}\,\underset{\sim}{U}^{+}\,\underset{\sim}{U}\,\underset{\sim}{\Psi}(1)\,\underset{\sim}{\Psi}^{+}(1')\,\underset{\sim}{U}^{+}$$
$$= \mathrm{Tr}\ \underset{\sim}{\bar{P}}\ \underset{\sim}{\bar{\Psi}}(1)\,\underset{\sim}{\bar{\Psi}}^{+}(1')$$

then for an orthonormal basis set $\{\Psi_i\}$, the diagonal elements of $\underset{\sim}{\bar{P}}$ are eigenvalues of the one electron density and the transformed basis functions $\{\bar{\Psi}_i\}$, called natural orbitals are eigenfunctions.

i.e. $$\hat{\rho}(1,1')\,\bar{\Psi}_m(1) = \int_{1'\to 1} \rho(1,1')\,\bar{\Psi}_m(1)\,d\tau_1$$
$$= \sum_n \lambda_n \bar{\Psi}_n(1) \int_{1'\to 1} \bar{\Psi}_n^{*}(1')\,\bar{\Psi}_m(1)\,d\tau_1$$
$$= \lambda_m \bar{\Psi}_m(1)$$

The λ's are interpreted as occupation numbers of the natural orbitals and to be quantum mechanically valid must lie in the region

$$0 \le \lambda_n \le 2$$ [29]

for a density described by doubly occupied orbitals. In the Hartree-Fock approximation, since $\hat{\rho}(1,1')$ is idempotent the only possible eigenvalues are 1 or 0 (or 2 or 0 for doubly occupied orbitals)

i.e. $$\hat{\rho}\psi = a\psi$$
$$\hat{\rho}^2\psi = a^2\psi$$

but $a = a^2$ so $a = 0$ or ± 1. Thus on diagonalizing an m dimensional matrix representative $\underset{\sim}{P}_I$ there must be N 1's and (N - m) zeros on the diagonal.

Four aspects of the N-Representability problem with regard to X-Ray Diffraction Data were studied.

1) Comparison of N-Representable and non N-Representable densities generated from the same structure factors, for the simple case of a one electron wave function.
2) Comparison of expectation values calculated from these two sets of densities.
3) A study of the effect on both densities of introducing a temperature factor into the structure factor and then into the basis functions.
4) The diagonalization of published $\underset{\sim}{P}$ matrices which were not constrained to be idempotent and examination of the eigenvalues obtained.

The basis set used consisted of orthonormal hydrogen 1s and 2s functions.

i.e.

$$\psi_1 = 1s = \left(\zeta^3/\pi\right)^{1/2} e^{-\zeta r}$$

$$\psi_2 = 2s = \left(\zeta^3/8\pi\right)^{1/2} e^{-\zeta r/2}\left(1 - \zeta/2 r\right)$$

One electron wave functions of the form

$$\Psi = c_1 \psi_1 + c_2 \psi_2$$

were defined by coefficients fulfilling the normalization constraint

$$c_1^2 + c_2^2 = 1$$

Model one electron density representations $\underset{\sim}{P}_C$ were calculated and used to construct a set of structure factors via

$$\rho(1,1') = Tr\ \underset{\sim}{c}^{+}\underset{\sim}{c}\ \underset{\sim}{\Psi}(1)\underset{\sim}{\Psi}(1') = Tr\ \underset{\sim}{P}_c\ \underset{\sim}{\Psi}(1)\underset{\sim}{\Psi}(1')$$

$$F(K) = \int \rho(1,1') e^{2\pi i K\cdot r} d^3r = Tr\ \underset{\sim}{P}_c \int \underset{\sim}{\Psi}(1) e^{2\pi i K\cdot r} \underset{\sim}{\Psi}(1') d\tau_1$$

$$= Tr\ \underset{\sim}{P}_c\ \underset{\sim}{f}(K)$$

where $\underset{\sim}{\Psi}$ are the hydrogenic basis functions with $\xi = 1.0$. See Appendix I for the calculation of $\underset{\sim}{f}(K)$.

The values of K, at which F(K) was determined were taken in the range

$$0 \leq \sin\theta/\lambda \leq 1.7\ \text{Å}^{-1}$$

where $K = 2\sin\theta/\lambda$. Experimental data, for example, obtained with Moko X rays, $\lambda = 0.7135$Å would be in the range

$$0 \leq \sin\theta/\lambda \leq \sim 1.4\ \text{Å}^{-1}$$

A least squares method was then used to obtain the matrices $\underset{\sim}{P}_I$ (idempotent) and $\underset{\sim}{P}_N$ (non-idempotent) by minimizing the functional

$$F = \sum_K w_K \left\{ F(K) - Tr\ \underset{\sim}{P}_{N\text{ or }I}\ \underset{\sim}{f}(K) \right\}^2 \quad \text{(II-1)}$$

with respect to the parameters in $\underset{\sim}{P}_N$ or $\underset{\sim}{P}_I$. The basis functions used in $\underset{\sim}{f}(K)$ were generally varied from the hydrogenic

functions by varying the scale factor, ξ. The simple two dimensional $\underset{\sim}{P}$ matrices have the form

$$\underset{\sim}{P}_I = \begin{pmatrix} p & \pm p^{1/2}(1-p)^{1/2} \\ \pm p^{1/2}(1-p)^{1/2} & (1-p) \end{pmatrix}$$

$$\underset{\sim}{P}_N = \begin{pmatrix} p & q \\ q & (1-p) \end{pmatrix}$$

Minimization of the functional with respect to $\underset{\sim}{P}_I$ amounts to solving a fourth order equation to obtain the one parameter p in $\underset{\sim}{P}_I$ which is in the range $o \leq p \leq 1$ and gives the minimum value for $\mathcal{H}$. Minimization of $\mathcal{H}$ with respect to p and q in $\underset{\sim}{P}_N$ results in a matrix equation

$$\underset{\sim}{A} = \underset{\sim}{B}^{-1}\ \underset{\sim}{C}$$

where $\underset{\sim}{B}(\omega_k, f(K))$, $\underset{\sim}{C}(\omega_k, f(k), F(K))$ and $\underset{\sim}{A}$ is a column matrix of p and q. The derivation of these equations is given in Appendix II. The weighting factor, ω_k, was taken as 1.0 for all values of k.

The eigenvalues of $\underset{\sim}{P}_N$ were routinely calculated by solving the secular equation

$$|\underset{\sim}{P}_N - \lambda \underset{\sim}{1}| = 0$$

As mentioned previously the eigenvalues of $\underset{\sim}{P}_I$ are necessarily 1 or 0. A deviation away from 1 or 0 in the eigenvalues of $\underset{\sim}{P}_N$ was taken to indicate a quantum mechanically invalid density.

All calculations except those referring to Table I were carried out in double precision on an IBM 370-168. When the value of the scale factor ξ was unity in both the basis functions used to construct the model density and the basis

functions used in the fitting procedures, the elements of the non-idempotent $\underset{\sim}{P}_N$ matrix were equal to the elements of the matrix representation of the model density to at least ten significant figures. The corresponding eigenvalues and point charge density evaluated between $o \leq r \leq 3.4$ a.u. were equal to those obtained from the model density to at least 13 significant figures and 14 decimal places respectively. The elements of the idempotent $\underset{\sim}{P}_I$ matrix were always equal to the elements of the model $\underset{\sim}{P}$ matrix to at least five significant figures. A crucial step in obtaining the one parameter, p, in $\underset{\sim}{P}_I$ involved solving a fourth order equation in p. The accuracy of the solution p, which gave the lowest value of the functional $\mathcal{F}$, was related to the number of decimal places to which the fourth order equation was satisfied.

Table I illustrates the correlation between the number of decimal places to which the fourth order equation was satisfied, and the number of significant figures to which the elements of the $\underset{\sim}{P}_I$ matrix and the corresponding expectation values were equal to those of the model density. The number given for the density is the smallest number of decimal places to which the non-idempotent and correct density agree. All densities are less than 1.0.

TABLE I

Correlation Between the Fourth Order Equation and the Accuracy of the $\underset{\sim}{P}_I$ Elements.

c_1	0 in fourth order equation	$\underset{\sim}{P}_I$ Elements	< >	$\rho(r)$
1.0	15	10	13	15
.99	11	8	8	9
.95	12	10	10	12
.90	15	10	14	15
.866	15	10	13	14
.85	14	10	12	13
.80	11	10	9	11
.75	9	8	7	8
.70	14	10	12	13
.65	11	10	9	11
.60	9	8	8	8
.55	8	6	6	7
.50	12	10	10	11
.5000439981	12	10	10	11
.45	10	8	8	9
.40	8	6	6	7
.35	12	10	10	11
.30	10	8	7	8
.25	8	5	4	5
.20	11	8	7	9
.15	9	6	6	7
.1410673598	8	6	5	6
.10	11	7	7	9

For explanation of Table see text.

The elements of the $\underset{\sim}{P}$ matrices were only printed out to ten decimal places and hence 10 in the $\underset{\sim}{P}_I$ elements column indicates an accuracy of at least ten significant figures. In the discussion of results the elements of the $\underset{\sim}{P}$ matrices are taken to be accurate to 5 significant figures. The expectation values are taken to be accurate to 4 significant figures. Eigenvalues are considered significant to five figures. Densities are judged to be accurate to at least four decimal places and functionals to six decimal places. It should be noted that none of the conclusions of this study depend upon the choice of one particular model density.

In the discussion of results, the following abbreviations are used.

$\underset{\sim}{P}_X$ where X = N, I or c

$\underset{\sim}{P}$ is the matrix representative of the one electron density.

$\underset{\sim}{P}_N$ and $\underset{\sim}{P}_I$ are obtained from the least squares fitting procedures without including the idempotency constraint and including the idempotency constraint respectively.

$\underset{\sim}{P}_C$ is the matrix representative of the model density.

ρ_X where X = N, I or c

ρ is the point charge density and is computed from

$$\rho = \mathrm{Tr}\ \underset{\sim}{P}\,\underset{\sim}{\Psi}\underset{\sim}{\Psi}^{+}$$

where $\underset{\sim}{\Psi}$ is a column matrix of the 1s and 2s hydrogenic basis functions with appropriate values of the scale factor ξ.

ξ_X where x = f or c

ξ is the scale factor in the hydrogenic basis functions

f refers to the basis functions used in the fitting procedure to obtain $\underset{\sim}{P}_N$ and $\underset{\sim}{P}_I$

c refers to the basis functions used to construct the model density.

"exact basis set" the 1s and 2s hydrogenic wave functions used to construct the model density.

"fitting basis set" the 1s and 2s hydrogenic wave functions used in the least squares fitting procedure to obtain $\underset{\sim}{P}_N$ and $\underset{\sim}{P}_I$.

Chapter III

In the simple case where the fitting basis set was identical to the exact basis set, $\underset{\sim}{P}_N = \underset{\sim}{P}_I = \underset{\sim}{P}_C$. The conclusion here was that if the system could be accurately described by a Hartree-Fock wave function and the basis set chosen could exactly fit this wave function, then the matrix representative $\underset{\sim}{P}$, of the one electron density obtained from a simple least squares fitting technique would necessarily be idempotent.

The crystallographic structure factor may be in error due to the scale factor s (equation I-6) which may be incorrectly determined in the conventional least squares refinement. To investigate the effect on $\underset{\sim}{P}_N$ and $\underset{\sim}{P}_I$ of such errors structure factors calculated as described in Chapter II, then varied by ±10% were used in the least squares equation (II-1).

The model density used was $0.641s^2 + 0.961s2s + 0.362s^2$. The fitting basis was identical to the exact basis. A similar study done by Clinton et al[24] (see also Appendix III) showed that the elements of $\underset{\sim}{P}_I$ changed less than the elements of $\underset{\sim}{P}_N$ as compared to $\underset{\sim}{P}_C$. This was thought to be due to the fact that $\underset{\sim}{P}_N$ could fit the data better and therefore would reflect the error in the structure factor more than $\underset{\sim}{P}_I$. Results here showed that although the percentage change in $\underset{\sim}{P}_I$ elements, as compared with those of $\underset{\sim}{P}_C$, was generally smaller than the percentage change in $\underset{\sim}{P}_N$ elements, the density obtained from $\underset{\sim}{P}_N$ was closer to the model density than that obtained from $\underset{\sim}{P}_I$. In the cases when the elements of $\underset{\sim}{P}_N$ were

closer to those of $\underset{\sim}{P}_C$, the density obtained from $\underset{\sim}{P}_I$ fit the model density most closely. On analysis the inverse correlation was seen to be due to a cancellation of errors, an increase in one element, being compensated by an appropriate decrease in another element. The densities were significantly different in the region $o \leq r \leq 1.2$ a.u., the maximum difference between ρ_N and ρ_I being 0.8%. Thus in terms of reproducing the model density when the structure factor was in error there was no obvious advantage in constraining $\underset{\sim}{P}$ to be idempotent. However, it was found that the eigenvalues of $\underset{\sim}{P}_N$ were not quantum mechanically valid when an error was introduced into the structure factor. This is shown in Table II.

Clearly, when dealing with experimental structure factors, the exact basis set will not be known. In order to simulate this situation the study was repeated using a fitting basis which was not identical with the exact basis, the difference being in the value of the scale factor ξ used in the hydrogenic basis functions. In some cases it was found that densities obtained from $\underset{\sim}{P}_N$ had negative values in certain regions of space. Clearly a negative density has no physical interpretation. A systematic study was thus undertaken to investigate the conditions under which such negative densities could occur.

TABLE II

Quantum Mechanically Invalid Eigenvalues for $P_{\sim N}$

ϵ	N_1
-10	1.0228
- 5	1.0076
- 1	1.0009
+ 1	0.9994
+ 5	1.0003
+10	1.0086

ϵ is the percentage error in the structure factor due to

$$F(K) \rightarrow SF(K)$$

N_1 is one eigenvalue of $P_{\sim N}$

Note that $N_1 + N_2 = 1$ due to the normalization constraint

This calculation was done in single precision and with

$$s = 1, \quad N_1 = 1.0000.$$

Model densities were constructed from hydrogenic basis functions (ξ = 1.0) and matrix representations $\underset{\sim}{P}_C$ as shown in Table III. $\underset{\sim}{P}_N$ and $\underset{\sim}{P}_I$ were obtained for fitting basis sets in which ξ varied from 0.6 - 1.6. Examples of negative densities obtained from $\underset{\sim}{P}_N$ are shown in Tables IV and V. No negative densities were obtained from $\underset{\sim}{P}_I$.

Analysis of the one electron density expression

$$\mathrm{Tr}\,\underset{\sim}{P}_N \Psi \Psi^+ = P_N(1,1)\psi_{1s}\psi_{1s} + 2P_N(1,2)\psi_{1s}\psi_{2s} + P_N(2,2)\psi_{2s}\psi_{2s}$$

with respect to the hydrogenic basis functions, revealed two possibilities for obtaining a negative density. If either of the diagonal elements of $\underset{\sim}{P}_N$ have large negative values or are negative in regions where the corresponding orbital product contribution is large, relative to the remaining product contributions, the density will be negative. Since a negative diagonal element in the $\underset{\sim}{P}$ matrix already implies an invalid quantum mechanical density, this is not surprising. More importantly, from a practical point of view, a large positive value for P_N (1,2) will result in a negative density in regions of space where the 1s2s orbital product has a relatively large negative value. Similarly a large negative value of P_N (1,2) could result in a negative density, depending on the relative contribution of each orbital product. P_N (1,2) is an independent parameter in the least squares fitting procedure and thus its only requirement is to attain a value which produces the best overall fit to the data. P_I (1,2), on the other hand, is constrained by the idempotency condition, to depend upon the diagonal elements and therefore the over-

TABLE III

Model Densities

c_1	$P_c(1,1)$	$P_c(1,2)$	$P_c(2,2)$
1.0	1.0000	0.0000	0.0000
0.99	0.9801	0.1397	0.0199
0.95	0.9025	0.2966	0.0975
0.90	0.8100	0.3923	0.1900
0.87+	0.7500	0.4330	0.2500
0.85	0.7225	0.4478	0.2775
0.80	0.6400	0.4800	0.3600
0.75	0.5625	0.4961	0.4375
0.70	0.4900	0.4999	0.5100
0.65	0.4225	0.4940	0.5775
0.60	0.3600	0.4800	0.6400
0.55	0.3025	0.4593	0.6975
0.50	0.2500	0.4330	0.7500
0.45	0.2025	0.4019	0.7975
0.40	0.1600	0.3666	0.8400
0.35	0.1225	0.3279	0.8775
0.30	0.0900	0.2862	0.9100
0.25	0.0625	0.2421	0.9375
0.20	0.0400	0.1960	0.9600
0.15+	0.0225	0.1483	0.9775
0.14+	0.0199	0.1397	0.9801
0.10	0.0100	0.0995	0.9900

+ see Table I for exact value of c_1

weighting which results in negative densities cannot occur.

It can be seen from Table VI, that for $\xi = 1.0$, the 1s2s orbital product becomes negative at 2.1 a.u. Furthermore between 3 and 4 a.u., all three orbital products are the same order of magnitude. Thus one would expect a negative density to occur in this region when

$$2\ P_N(1,2) > P_N(1,1) + P_N(2,2)$$

$$\text{i.e.} \qquad 2\ P_N(1,2) > 1.0 \qquad \text{(III-1)}$$

Obviously when ξ is less than 1.0 in the fitting basis, a negative density will not occur until larger values of r, but for ξ greater than 1.0 the distance at which the first negative density may occur will be smaller. This is illustrated by comparing Tables VI and VII. Initial results (Table IV) indicated that condition (III-1) was a useful guideline in predicting negative densities, when the basis functions used in the fitting procedure were more diffuse than those used in the model density. A more comprehensive study (Table V) revealed that as the fitting basis functions became closer to the exact basis functions, negative densities were sometimes obtained when the off diagonal elements of $\underset{\sim}{P}_N$ did not appear excessively large. In regions of space where the 1s2s orbital product is negative, but all orbital products are not the same order of magnitude (see Table VII). there is no simple relationship between the elements of $\underset{\sim}{P}_N$ which allows the prediction of negative densities. When one

TABLE IV

Examples of negative densities obtained when the idempotency constraint is omitted.

c_1	ξ_f	$\rho_N(r)$	r	$P_N(1,1)$	$P_N(1,2)$	$P_N(2,2)$	N_1	R
0.99	0.6	-.0004	4.7	.4681	2.068	.5319	2.57	.1031
0.866	0.7	-.0005	4.1	.4811	1.534	.5187	2.03	.1313
0.80	0.7	-.0004	4.1	.4391	1.400	.5609	1.90	.1399
0.60	0.8	-.0002	3.6	.3600	.7278	.6399	1.24	.0987
.14	1.6	-.0053	1.2	-.2241	.4497	1.224	1.35	.3035

c_1 describes the model density (Table II)

ξ_f is the scale factor used in the fitting basis functions

$\rho_N(r)$ is the point charge density obtained from $\mathrm{Tr}\, \underset{\sim}{P_N}\, \underset{\sim}{\Psi}\, \underset{\sim}{\Phi}^{+}$

r is in atomic units

N_1 is an eigenvalue of $\underset{\sim}{P}_N$

$\sin\theta/\lambda$ ranges from 0 - 0.8, in increments of .02.

$$R = \left\{ \sum_{\kappa} \left(F(\kappa) - \mathrm{Tr}\, \underset{\sim}{P}\, \underset{\sim}{f}(\kappa) \right)^2 \Big/ \sum_{\kappa} F(\kappa)^2 \right\}^{1/2}$$

TABLE V

Examples of negative densities obtained when the idempotency constraint is omitted.

c_1	ξ_f	$\rho_N(r)$	r	$P_N(1,1)$	$P_N(1,2)$	$P_N(2,2)$	N_1	R
0.9	.95	-.0001	3.7	.7719	.5563	.2281	1.119	.0141
0.8	.95	-.0001	3.4	.6119	.6131	.3881	1.123	.0172
0.7	.95	-.0001	3.2	.4741	.5972	.5259	1.098	.0199
0.6	.95	-.0001	3.1	.3750	.5427	.6430	1.061	.0225
0.3	1.05	-.0001	2.3	.0625	.3099	.9375	1.036	.0276
0.2	1.05	-.0002	2.2	.0035	.2426	.9964	1.053	.0283
0.1	1.05	-.0003	2.0	-.0343	.1654	1.034	1.05	.0282
0	1.05	-.0003	1.9	-.0507	.0811	1.051	1.053	.0406

See Table IV for explanation of symbols.

TABLE VI

Numerical values for the orbital products of the hydrogenic 1s and 2s wave functions (ξ=1.0) at various values of r

r (a.u.)	1s1s	1s2s	2s2s
0	.3183	.1125	.0398
.4	.1430	.0494	.0171
.8	.0643	.0203	.0064
1.2	.0289	.0074	.0019
1.6	.0130	.0020	.0003
2.0	.0058	0.0000	0.0000
2.1	.0048	-.0002	.00001
2.4	.0026	-.0006	.0001
2.8	.0012	-.0007	.0004
3.2	.0005	-.0006	.0006
3.6	.0002	-.0004	.0007
4.0	.0001	-.0003	.0007
4.4	.0001	-.0002	.0007
4.8	.0000	-.0001	.0006

$$1s1s = \frac{\xi^3}{\pi} e^{-2\xi r}$$

$$1s2s = \frac{\xi^3}{2\sqrt{2}\pi} e^{-3/2\,\xi r}\left(1 - \xi r/2\right)$$

$$2s2s = \frac{\xi^3}{8\pi}\left(1 - \xi r/2\right)^2 e^{-\xi r}$$

TABLE VII

Numerical values for the orbital products of the hydrogenic 1s and 2s wave functions (ξ=1.05) at various values of **r**

r(a.u.)	1s1s	1s2s	2s2s
0	.3685	.1303	.0461
0.2	.2421	.0851	.0299
0.4	.1591	.0548	.0189
0.6	.1045	.0347	.0115
0.8	.0687	.0214	.0067
1.0	.0451	.0128	.0036
1.2	.0296	.0073	.0018
1.4	.0195	.0038	.0007
1.6	.0128	.0017	.0002
1.8	.0084	.0004	.00002
2.0	.0055	-.0003	.00001
2.2	.0036	-.0006	.0001
2.3	.0029	-.0007	.0002
2.4	.0024	-.0008	.0003
2.5	.0019	-.0008	.0003

see Table V for explanation of symbols.

attempts to fit model densities very close to hydrogenic 1s or 2s functions (ζ=1.0), with basis functions which are more contracted, negative densities do occur due to overweighting of the appropriate orbital product which produces a negative diagonal element due the normalization constraint.

From these results a general conclusion may be drawn that if the basis functions contain nodes there is a possibility of obtaining negative density if the idempotency constraint is omitted. It is noted that Slater-type orbitals are often used for this type of calculation. Although the radial component of these functions contain no nodes the spherical harmonics contain Legendre functions which possess angular nodes.

One interesting consequence of the above study could occur in the qualitative interpretation of population asphericity maps. These are constructed from the difference between the molecular density obtained via a least squares fitting technique without the idempotency constraint and the sum of spherical densities over all the atoms in the molecule. Thus positive and negative regions indicate, respectively a build up or decrease of electron density in that region, during molecular formation. Since the least squares method gives the best fit to the data, one would expect negative densities to occur in regions where the true molecular density was small. Misinterpretation could result if the true molecular density was larger than the atomic density in this region but the molecular density obtained from the fitting procedure was

negative. Such a misinterpretation of course could only occur if the corresponding molecular density map was not plotted separately along with the population asphericity map. It should be pointed out that the effect of such a situation on an asphericity map would not be drastic, but merely shift the positive contours, for example, in the lone pair region, slightly farther away from the nucleus or appear as an obvious discrepancy.

Comparison of Tables IV and V shows that the eigenvalues obtained from the non-idempotent one electron density are closer to 1.0 when the fitting basis functions approach the exact basis functions. This is illustrated more clearly in Table VIII. From this table one could also conclude that the lowest value of the functional,

$$\mathcal{F} = \sum_k \omega_k \left[F(k) - \mathrm{Tr}\, P f(k) \right]^2$$

corresponds to the "most quantum mechanically valid" eigenvalue or the "most N-Representable density". However, calculations undertaken as an extension of a study done by Clinton and Massa[24] (see Appendix III), showed that this was not true when the basis functions used were fundamentaly different from the functions used to construct the model density. In this case the model density was that termed by Stewart as "the best spherical density" for a hydrogen atom in the hydrogen molecule[30]. This density originates from minimizing the quantity

$$\mathcal{E} = \int \left[2\rho - (\rho_a + \rho_b) \right]^2 d\tau$$

TABLE VIII

Eigenvalues and functionals for the non-idempotent density obtained by fitting hydrogenic basis functions (ξ_f) to the model density.

$$\rho = 0.64\ 1s^2 + 0.96\ 1s2s + 0.36\ 2s^2 \quad (\xi = 1.0)$$

ξ_f	N_1	$\mathcal{F}$
0.98	1.0388	.00019
0.99	1.0192	.00005
1.0	1.0000	D - 29
1.01	.9811	.00004
1.02	.9636	.00017

N_1 = eigenvalue for non-idempotent density

$$\mathcal{F} = \sum_k \omega_k \left[F(k) - \mathrm{Tr}\, \underset{\sim}{P}_N\, f(k) \right]^2$$

$0 \leq \sin\theta/\lambda \leq 1.7176\ \text{Å}^{-1}$ Stewart et al.[30]

where

$$\rho = \left(2/R\right)^3 \left(1/2\pi\right) \exp\left(-\alpha\xi\right) \sum_{k,j} a_{kj}\, \xi^k \eta^j$$

and is a modified form of the Kolos Roothaan wave function for H_2. The fitting basis functions used were again the hydrogenic 1s and 2s functions and the scattering factors for ρ_a were taken from Stewart et al[30]. Table IX shows that the "most quantum mechanically valid" eigenvalue for the non-idempotent density occurs for a value of $\xi = 1.09$ in the basis functions. This does not correspond to the minimum functional which occurs for a value of $\xi = 1.13$. This implies that parameterization of ξ in a least squares fitting procedure would not necessarily lead to the "most N-Representable density".

TABLE IX

Eigenvalues and functionals for the non-idempotent density obtained by fitting hydrogenic basis functions to Stewart's "best spherical density" for a Hydrogen Atom.

ξ_f	N_1	$\mathcal{H}$
1.08	1.0055	.00047
1.09	1.0004	.00033
1.10	.9967	.00022
1.11	.9945	.00015
1.12	.9937	.00011
1.13	.9942	.00010
1.14	.9960	.00012

For explanation of symbols see Table VIII

Chapter IV

Although the overall fit of the calculated structure factor to the true structure factor, as judged by the functional

$$\mathcal{F} = \sum_{k} \left[\mathrm{Tr}\, \underset{\sim}{P}\, \underset{\sim}{f}(k) - F(k) \right]^2 \qquad \text{(IV-1)}$$

was always better for the non-idempotent than the idempotent density, due to the larger number of parameters, an important criterion for any density is its ability to predict expectation values. With this in mind a series of calculations was undertaken, using model densities consisting of idempotent $\underset{\sim}{P}$ matrix representations (Table III) in the 1s and 2s hydrogenic basis functions (ξ = 1.0). 1s and 2s hydrogenic basis functions with varying values of ξ_f were then fit to structure factors, derived from the model densities, in the manner previously described, to obtain two matrices, i.e. $\underset{\sim}{P}_I$, resulting from coupling idempotency and normalization constraints with the least squares fitting procedure and $\underset{\sim}{P}_N$ resulting from only the normalization constraint being included in the least squares fitting equations.

Expectation values were calculated from

$$\langle A \rangle = \mathrm{Tr}\, \underset{\sim}{P}\, \underset{\sim}{A} \qquad \text{(IV-2)}$$

where the elements of the matrix $\underset{\sim}{A}$ are given by

$$A_{ij} = \int \psi_i^* \hat{A}\, \psi_j \, d\tau$$

The operators considered were functions of r, but not of the angular coordinates, which reduced the matrix elements to

$$A_{ij} = \int_0^\infty \psi_i^*(r)\, \hat{A}\, \psi_j(r)\, r^2\, dr$$

since the spherical harmonics of the 1s and 2s hydrogenic wave functions are identical and normalized. The integrals required were evaluated analytically and the generalized expressions for the matrix elements are shown in Table X. The expectation values derived from equation (IV-2) using the matrix representation and basis functions of the model density were termed the correct expectation values. These were compared with expectation values, predicted from (IV-2) with $\underset{\sim}{P}_N$ and $\underset{\sim}{P}_I$ and the fitting basis functions. The results showed that the closeness of the predicted expectation values to the correct expectation values was not directly correlated with the best fit of the calculated structure factors to the model structure factors. In other words there were many cases in which the idempotent matrix predicted better expectation values than the non-idempotent matrix, even though the value of the functional was always smallest for the latter. In order to understand this the following points must be taken into account. Firstly, the lower value of the functional for P_N does not mean that at every value K, the difference

$$\Delta = \mathrm{Tr}\,\underset{\sim}{P}\,\underset{\sim}{f}(k) - F(k)$$

is smaller for $\underset{\sim}{P}_N$. There may, for example, be some regions in which $\underset{\sim}{P}_N$ fits the data better than $\underset{\sim}{P}_I$ and others in which $\underset{\sim}{P}_I$ fits more closely than $\underset{\sim}{P}_N$, the difference between the values of Δ for $\underset{\sim}{P}_N$ and $\underset{\sim}{P}_I$ being smaller in the latter region. Secondly, there existed correlations between some of the expectation values studied and the goodness of the fit to the density in certain regions of space. For instance, as intuitively expected, there was a direct correlation between

TABLE X

Matrix elements of the operators, in the hydrogenic basis set, used in the calculation of expectation values.

$\hat{r}^n \qquad -2 \leq n \leq 2$

$$r^n(1,1) = 4\xi^3(2+n)! \,/\, (2\xi)^{3+n}$$

$$r^n(1,2) = \sqrt{2}\,\xi^3(n+2)!\,[1-(n+3)/3] \,/\, (\tfrac{3}{2}\xi)^{n+3}$$

$$r^n(2,2) = (\xi^3/2)\left[\frac{(n+2)!}{\xi^{n+3}} + \frac{\xi^2}{4}\frac{(n+4)!}{\xi^{n+5}} - \xi\frac{(n+3)!}{\xi^{n+4}}\right]$$

$\hat{E}$ - Total Energy

$$E(1,1) = \tfrac{1}{2}\xi(\xi-2)$$

$$E(1,2) = \frac{4\sqrt{2}}{27}\xi(\xi-1)$$

$$E(2,2) = \tfrac{1}{8}\xi(\xi-2)$$

$\hat{T}$ - Kinetic Energy

$$T(1,1) = \tfrac{1}{2}\xi^2$$

$$T(1,2) = \frac{4\sqrt{2}}{27}\xi^2$$

$$T(2,2) = \tfrac{1}{8}\xi^2$$

$\langle 1/r \rangle$, or $\langle 1/r^2 \rangle$ for most contracted model densities, and the best fit to the density at values of r close to the nucleus, i.e. the matrix representation which predicted $\langle 1/r^n \rangle$ most closely, as compared to the correct $\langle 1/r^n \rangle$, was found to be the representation of that density which fit the model density most closely at small values of r. Finally, as was discussed in Chapter I, the higher angle scattering data contains a relatively larger contribution from the more contracted inner density. (see Figure I). Analysis of the results showed that where Δ was smaller for $\underset{\sim}{P}_I$ at larger scattering angles, both the fit to the model density at small values of r and the fit of $\langle 1/r^n \rangle$ to the correct expectation value, were closer for $\underset{\sim}{P}_I$ than $\underset{\sim}{P}_N$. This is illustrated in Table XI and Figure II.

Correlations between $\langle E \rangle$, $\langle T \rangle$ and $\langle 1/r \rangle$ were also found as shown in Tables XII and XIII. To some extent the average value of the kinetic energy may be expected to be correlated with the best fit to the inner density, since for a spherical density the largest contributions to the average value are at smaller values of r. The value of ξ in the basis set used to fit structure factors derived from the model densities shown in Table XII, was varied between 0.95 and 1.05. It is seen that in this region the relationship

$$\langle E \rangle = \langle T \rangle - \langle 1/r \rangle$$

produces a correlation between the three expectation values. This correlation and also the invariance to changes in ξ_f of the type of $\underset{\sim}{P}$ matrix which predicted a particular expectation

FIGURE 1

Fourier Transforms of the Hydrogenic Orbital Products

a) $\int 1s1s\, e^{2\pi i \vec{k}\cdot\vec{r}}\, d^3\vec{r}$

b) $\int 2s2s\, e^{2\pi i \vec{k}\cdot\vec{r}}\, d^3\vec{r}$

c) $\int 1s2s\, e^{2\pi i \vec{k}\cdot\vec{r}}\, d^3\vec{r}$

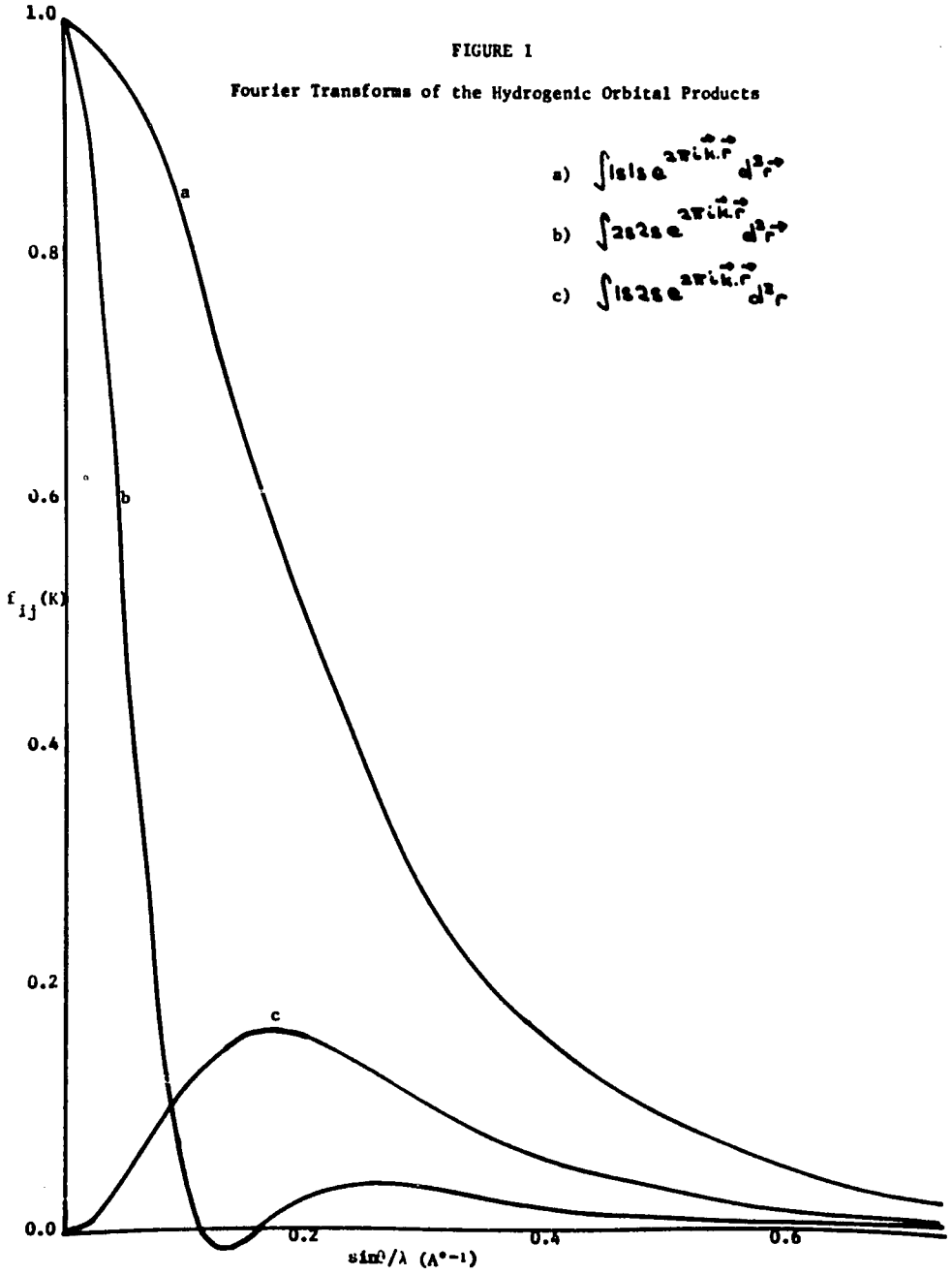

TABLE XI

Correlation between the fit to high scattering angle data and $\langle 1/r^n \rangle$

$c_1 = 0.141, \quad \xi_f = 1.05$

	P_N	P_I	P_c
$\langle 1/r \rangle$	.3329	.3301	.3234
$\langle 1/r^2 \rangle$	.5091	.4799	.4604

Δ_{PN}	Δ_{PI}	$\sin\theta/\lambda$
0.0000	0.0000	0.0
0.0176	0.0257	0.04
0.0084	0.0224	0.08
0.0129	-0.0051	0.12
0.0126	-0.0132	0.16
0.0036	-0.0088	0.20
0.0033	-0.0033	0.24
0.0064	0.0001	0.28
0.0071	0.0018	0.32
0.0067	0.0023	0.36
0.0058	0.0024	0.40
0.0049	0.0022	0.44
0.0040	0.0019	0.48
0.0033	0.0016	0.52
0.0027	0.0014	0.56
0.0022	0.0011	0.60
0.0018	0.0010	0.64
0.0015	0.0008	0.68
0.0012	0.0007	0.72

$\Delta = \mathrm{TrPf}(K) - F(K), \quad |K| = 2\sin\theta/\lambda$

FIGURE II

Comparison of Densities close to the nucleus,

$c_1 = 0.141$, $\xi_1 = 1.05$

a) $Tr\ \underset{\sim}{P}_N\ \underset{\sim}{\psi}(r)\underset{\sim}{\psi}^+(r)$

b) $Tr\ \underset{\sim}{P}_2\ \underset{\sim}{\psi}(r)\underset{\sim}{\psi}^+(r)$

c) $Tr\ \underset{\sim}{P}_0\ \psi(r)\psi^+(r)$

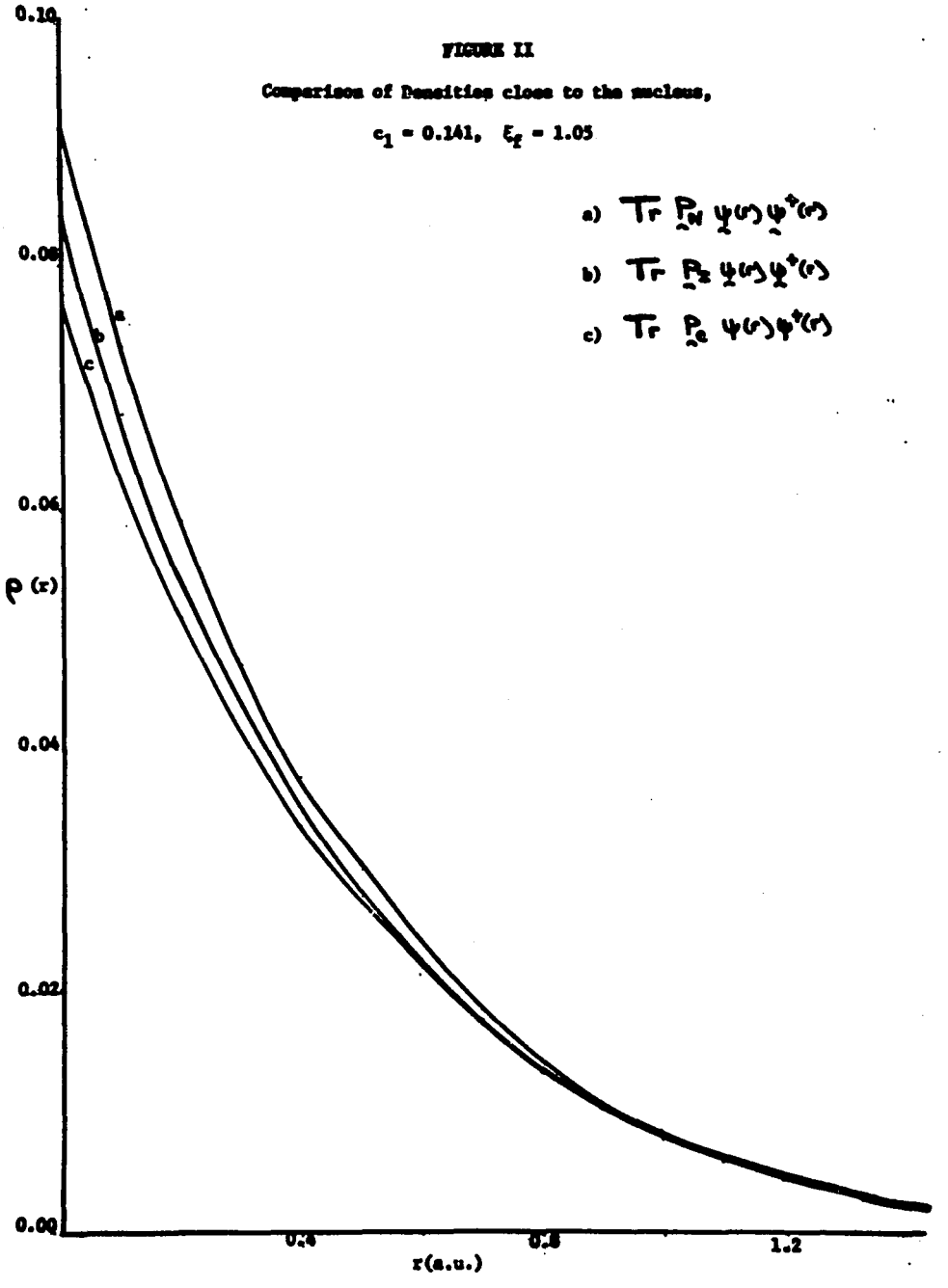

TABLE XII

The trends in expectation values

a) $o \leq \sin\theta/\lambda \leq 0.8\ A^{o-1}$ in increments of 0.02	b) $o \leq \sin\theta/\lambda \leq 0.77°A_{30}$ Stewart's values.
$1.0 \geqslant c_1 \geqslant 0.95$ No observable trends	c_1 0.99 no observable trend
$0.9 \geqslant c_1 \geqslant .45$ $\langle r \rangle$ $\langle r^2 \rangle$ predicted more closely by P_I $\langle E \rangle$ $\langle T \rangle$ $\langle 1/r \rangle$ $\langle 1/r^2 \rangle$ predicted more closely by P_N.	0.866 $\langle r \rangle$ $\langle r^2 \rangle$ predicted 0.800 more closely by P_I 0.600 $\langle E \rangle$ $\langle T \rangle$ $\langle 1/r \rangle$ $\langle 1/r^2 \rangle$ predicted more closely by P_N.
$0.4 \geqslant c_1 \geqslant 0.1$ $\langle E \rangle$ $\langle T \rangle$ $\langle 1/r \rangle$ $\langle 1/r^2 \rangle$ predicted more closely by P_I. $\langle r \rangle$ $\langle r^2 \rangle$ predicted more closely by P_N.	0.500^+ $\langle E \rangle$ $\langle T \rangle$ $\langle 1/r \rangle$ $\langle 1/r^2 \rangle$ 0.141^+ predicted more closely by P_I. $\langle r \rangle$ $\langle r^2 \rangle$ predicted more closely by P_N.
c_1 was varied by 0.05 to give model densities shown in Table III.	+ for exact c_1 used see Table I.

In both calculations ξ_f was varied between 0.95 and 1.05 in increments of .01. The trends displayed are for this range of ξ_f.

TABLE XIII

The correlation between <E>, <T> and <1/r> for a given model density and varying values of ξ_f.

	<1/r>		-<E>		<T>	
ξ_f	P_N	P_I	P_N	P_I	P_N	P_I
.95	.7079	.7040	.2690	.2777	.4388	.4263
.97	.7133	.7110	.2653	.2708	.4480	.4402
.99	.7186	.7178	.2618	.2637	.4568	.4541
1.0	.7211		.2600		.4611	
1.01	.7236	.7244	.2583	.2563	.4654	.4681
1.03	.7285	.7309	.2549	.2487	.4736	.4822
1.05	.7332	.7372	.2517	.2409	.4815	.4963

$c_1 = 0.6, \quad 0 \leq \sin\theta/\lambda \leq 0.8, \quad 0.02\ \mathring{A}^{-1}$

The correct expectation values are those given by $\xi_f = 1.0$. P_N predicts better values of <E>, <T>, <1/r> for this model density.

value most closely for a given model density, (see for e.g. Table XIII) were no longer apparent for very contracted model densities. No obvious reasons for the breakdown of this invariance could be found. This was also the case when ξ_f was allowed to vary farther away from 1.0 ($0.6 \leq \xi_f \leq 1.6$). Cases in which a particular $\underset{\sim}{P}$ matrix predicted the best value of <1/r> and <T> but not <E> were due to a cancellation of errors. An example is shown in Table XIV.

The scattering angles at which X-ray intensity is observed, which define the magnitude of $\vec{K}$, are of course fixed when X-rays are diffracted by a crystal. The fourier transform of a single spherical density is, however, continuous and therefore the values of $|\vec{K}|$ which may be chosen in these calculations are to a certain extent arbitrary. In order to simulate a situation in which results would be taken from a crystallographic experiment, the maximum value of $|\vec{K}|$ was taken close to the maximum value for which intensity could be observed e.g. for MoKα radiation $(\sin\theta/\lambda)_{max} \sim 1.4$ A°$^{-1}$. The values of $|\vec{K}|$ originally used were taken from Stewart et al.[30] It was noted in this study however that for values of $\sin\theta/\lambda$ >0.8 A°$^{-1}$ there was no contribution to the functional, to five significant figures, from the quantity

$$(\mathrm{Tr}\ \underset{\sim}{P}\ \underset{\sim}{f}(K) - F(K))^2$$

for either $\underset{\sim}{P}_I$ or $\underset{\sim}{P}_N$. The study was repeated using only values of $\sin\theta/\lambda$ up to 0.77 A°$^{-1}$. The trends in the expectation values remained the same and the elements of the $\underset{\sim}{P}$ matrices

TABLE XIV

The breakdown of the correlation between <E>, <T> and <1/r> for a large variation in ξ_f.

	<1/r>		-<E>		<T>	
ξ_f	P_N	P_I	P_N	P_I	P_N	P_I
.6	.8143	.6304	.4197	.4187	.3945	.2118
.8	.9272	.8351	.4061	.4562	.5211	.3789
1.0	.9939		.4062		.5877	
1.2	1.030	1.020	.4344	.4817	.5957	.5385
1.4	1.047	1.054	.4887	.4575	.5585	.5963

$c_1 = 0.866$

$\sin\theta/\lambda$ range 0.0 - 0.8, 0.02 $\mathring{A}^{-1}$

$\langle E \rangle = \langle T \rangle - \langle 1/r \rangle$

at $\xi = 0.6$

$\langle E \rangle_{PN} = .3945 - .8143 = .4198$

$\langle E \rangle_{PI} = .2118 - .6304 = .4186$

$\langle E \rangle_{c} = .5877 - .9939 = .4062$

Although $\langle T \rangle_{PN}$ and $\langle 1/r \rangle_{PN}$ are closer to the correct expectation values, the difference between them is larger than the corresponding difference for P_I.

differed from those in the previous study by at most .0003. Another study was undertaken in which $\sin\theta/\lambda$ was varied from 0 - 0.8 $\mathring{A}^{-1}$ in steps of 0.02 $A^{\circ -1}$. The trends in the expectation values remained the same for all model densities studied previously, except for $c_1 = 0.5$, in which the trends were reversed. See Table XII. This was due to the fact that the higher angle scattering data was now fit more closely by $\underset{\sim}{P}_N$. Thus the choice and/or number of data points chosen in each region may determine which $\underset{\sim}{P}$ matrix predicts which expectation value most closely for some model densities. However, it is clear that the idempotent matrix, in all the model densities studied with different data sets, predicts some expectation values more closely than the non-idempotent matrix. This fact questions the validity of the assumption that the density which produces the best fit to the crystallographic data, as judged by the functional (IV-1), is the best possible density. An important point to note in connection with this, is that when the density was not constrained to be idempotent in the least squares fitting technique and subsequently used to calculate <E>, the variational principle was sometimes violated. Examples are shown in Table XV. Examination of the matrix elements of $\underset{\sim}{E}$, shows that for $\xi > 1.0$ the E(1,2) term is positive. However a large negative value for P(1,2) or a large positive value for P(1,1) will result in a large negative energy. As pointed out in Chapter II, for a one electron system, a diagonal $\underset{\sim}{P}$ element of magnitude greater than 1.0, necessarily gives rise to a negative diagonal element which is readily recognizable as quantum mechan-

TABLE XV

Examples of Violation of the Variational Principle

c_1	ξ_f	$\langle E \rangle_{PN}$	PN(1,1)	PN(1,2)	PN(2,2)	N_1	R
1.0	1.01	-.5022	1.006	-.0298	-.006	1.006	.0016
.99	1.04	-.5013	1.006	-.0134	-.006	1.006	.0068
	1.6	-.7166	1.086	-.9346	-.086	1.603	.0042
.866	1.5	-.5231	.9098	-.5521	.0902	1.188	.0643
	1.6	-.5605	.9091	-.6522	.0909	1.270	.0669

c_1 defines the model density

ξ_f is the value of ξ in the basis functions used to fit the data.

N_1 is an eigenvalue of $\hat{\rho}_N$. $N_1 + N_2 = 1.0$

$$R = \left\{ \sum_K \left(F(K) - \mathrm{Tr}\, \underline{\rho}_N \underline{f}(K) \right)^2 \Big/ \sum_K F(K)^2 \right\}^{1/2}$$

ically invalid. The more interesting situation is again, that in which it is the independent parameter $P_N(1,2)$ which causes the violation of the variational principle. The eigenvalues associated with the $\underset{\sim}{P}_N$ matrices in Table XIV are quantum mechanically invalid, although the values for the R factors are reasonable.

Since the scattering of X-rays from a crystal is a one electron property and the intensity of scattered X-rays is related to the structure factor via $I(\vec{K}) = F(\vec{K})\ F(\vec{K})^*$ the effect of using an idempotent and a non-idempotent density to calculate the expectation values $\langle F(K) \rangle$ was next examined. Structure factors were calculated in the usual manner for values of $\sin\theta/\lambda$ up to 0.8 $A^{\circ -1}$, from the model densities shown in Table III. $\underset{\sim}{P}_N$ and $\underset{\sim}{P}_I$ were then generated from the appropriate least squares fitting techniques, but only the low scattering angle data i.e. $(\sin\theta/\lambda)_{max} = .36\ \mathring{A}^{-1}$, was used in the fitting procedure. The densities so obtained were then used to calculate $\langle F(K) \rangle$ for the larger scattering angles, i.e. $0.38 \leq \sin\theta/\lambda \leq 0.8\ \mathring{A}^{-1}$, via

$$\text{Tr}\ \underset{\sim}{P}\ \underset{\sim}{f}(K) = \langle F(K) \rangle$$

Instead of comparing these predicted expectation values with the structure factors derived from the model density at each value of |K|, the predicted functionals

$$\text{predicted} = \sum_{K=0.38}^{0.8} \left[F(K) - \text{Tr}\ \underset{\sim}{P}\ \underset{\sim}{f}(K) \right]^2$$

obtained for $\underset{\sim}{P}_N$ and $\underset{\sim}{P}_I$ were compared. The results showed that the non-idempotent matrix, which always gave a lower

functional from the actual fitting procedure, did not necessarily give the smallest value for the predicted functional. Some examples are shown in Table XVI. When ξ_f was varied between 0.95 and 1.05 in increments of 0.01 $\mp$ predicted was correlated with $\langle 1/r^n \rangle$, $\langle T \rangle$ and $\langle E \rangle$ which were routinely generated from the matrices obtained from the low scattering angle fit. The trend in these expectation values was the same as that in Table XII. As before, when the range of ξ_f was expanded i.e. $0.6 \leq \xi_f \leq 1.6$, increments of 0.1, the trends were not so well defined. However in all cases the smallest value of the predicted functional was correlated with the closest fit of $\langle 1/r^n \rangle$ to $\langle 1/r^n \rangle_{correct}$. In the previous study the best value of $\langle 1/r^n \rangle$ was predicted by that matrix which gave the smallest value

$$\Delta = \mathrm{Tr}\, \underset{\sim}{P}\, \underset{\sim}{f}(K) - F(K)$$

for all larger values of $|K|$. This would suggest that the matrix which gives the lowest predicted functional in this study does indeed predict expectation values, $\langle F(K) \rangle$, which fit the correct structure factor more closely at each value of K, for the larger scattering angles.

TABLE XVI

Comparison of Predicted Functionals

$c_1 = .141$

	R values		Functionals		Predicted Functionals	
ξ_f	P_N	P_I	P_N	P_I	P_N	P_I
.95	.0256	.0353	.00157	.00298	.00024	.00005
.97	.0155	.0211	.00057	.00107	.00009	.00002
1.02	.0105	.0105	.00026	.00047	.00004	.00001
1.05	.0264	.0348	.00166	.00290	.00030	.00005

$c_1 = .800$

	R values		Functionals		Predicted Functionals	
ξ_f	P_N	P_I	P_N	P_I	P_N	P_I
1.3	.0518	.0744	.01714	.03538	.01495	.00288
1.4	.0612	.0736	.02393	.03459	.02272	.00750
1.5	.0686	.0753	.03006	.03620	.03045	.01351
1.6	.0746	.0783	.03558	.03917	.03787	.02017

R is defined in Table XIV.

Functionals obtained from $\sum_{0 \leq \sin\theta/\lambda \leq 0.36\ \text{Å}^{-1}} [T - P_{\xi_f}(k) - F(k)]^2$

Predicted functionals obtained by calculating the above difference in the range $.38 \leq \sin\theta/\lambda \leq 0.8\ \text{Å}^{-1}$

Chapter V

The results reported thus far in this study have neglected any effects due to thermal motion of the atoms, which is of course occurring in a real crystal. Any attempt to obtain the electron density distribution from experimental data must take account of the fact that X-rays are scattered by a thermally smeared rather than a static density. Assuming that the spherical electron density vibrates with the nucleus, then for a displacement $\vec{\Delta r}$ of the nucleus from its equilibrium position

$$F(\vec{K}) = \int \rho(\vec{r})\, e^{2\pi i \vec{k}\cdot\vec{r}}\, d^3\vec{r}\; e^{2\pi i \vec{k}\cdot\vec{\Delta r}}$$

$$= F_0(\vec{k})\, e^{2\pi i k\cdot\vec{\Delta r}}$$

where $F_0(\vec{k})$ is the structure factor obtained from the static density. Since the atomic vibration frequency is much smaller than the X-ray frequency the average $F(\vec{K})$ over all positions $\vec{\Delta r}$ gives the appropriate structure factor for a thermally smeared density. After simple mathematical manipulation, to a first approximation the expression becomes

$$\langle F(k) \rangle = F_0(\vec{k})\, e^{-2\pi^2 |\vec{k}|^2 \langle u^2 \rangle}$$

where $\langle u^2 \rangle$ is the mean square amplitude of atomic vibration. The exponential factor

$$e^{-B\sin^2\theta/\lambda^2}$$

with

$$B = 8\pi^2 \langle u^2 \rangle$$

is called the Debye Waller factor. Although the situation in a crystal is more complex, the structure factor described a-

bove may be derived by assuming all atoms to be vibrating in the same harmonic isotropic manner. The simple approach taken in this study was to test whether appropriate modification of the methods previously described would allow the static density to be obtained from such a structure factor and to determine the effect, if any, of the idempotency constraint.

Clearly, in the case where the exact basis functions are used, minimization of the functional

$$\mathcal{F} = \sum_k \left[F_o(k) e^{-B\sin^2\theta/\lambda^2} - \mathrm{Tr}\, \underset{\sim}{P}\, \underset{\sim}{f}(k) e^{-B\sin^2\theta/\lambda^2} \right]^2$$

with respect to $\underset{\sim}{P}$ will reproduce the matrix representation of the model static density. This is equivalent to multiplying each basis function by the factor $e^{-B/2\sin^2\theta/\lambda^2}$ However since the exponential term can be extracted from the square this modification essentially introduces a weighing factor into the functional

$$\text{i.e.} \quad \mathcal{F} = \sum_k e^{-B/2\sin^2\theta/\lambda^2} \left[F_o(k) - \mathrm{Tr}\, \underset{\sim}{P}\, \underset{\sim}{f}(k) \right]^2$$

Although this has no effect when the exact basis functions are used it will, in the case of non-exact basis functions emphasize the fit to low scattering angle data. Structure factors were calculated, as previously described, from model densities with $0.2 \leq c_1 \leq 1.0$, where c_1 was varied in increments of 0.2. These structure factors were multiplied by the Debye Waller factor with B = 4.0 $A^{\circ 2}$. Hydrogenic 1s and 2s basis functions modified by the Debye Waller factor with B = 2.0 $A^{\circ 2}$, and with varying values of ξ_f were then used in the least squares fitting procedures to obtain the

idempotent and non-idempotent matrices $\underset{\sim}{P}_I$ and $\underset{\sim}{P}_N$. Calculations were also carried out using the same structure factors but with no modification of the hydrogenic basis functions. As expected it was found that modification of the basis functions by the appropriate Debye Waller factor resulted in a density which was closer to the model "static" density, than that obtained when there was no modification. This was true for both the idempotent matrix representation $\underset{\sim}{P}_I$ and the non-idempotent matrix representation $\underset{\sim}{P}_N$ and is illustrated in Figures III and IV. The expectation values were also predicted more closely when the basis functions were modified. An example is shown in Table XVII. When the basis functions were modified in order to account for the Debye Waller factor introduced into F(K), the trends as regards whether the idempotent or the non-idempotent matrix representation predicted the better expectation value for a particular model density were the same as those in Table XIIa. The results in Table XII(a) were obtained by simply fitting Tr $\underset{\sim}{P}\ \underset{\sim}{f}(K)$ to the structure factor calculated from the static model density and there was no consideration of thermal motion at all. However the trends in the expectation values when the basis functions were not modified differed from both these results in that $\langle 1/r \rangle$ was predicted more closely for the more contracted model densities (c_1 = 1.0, 0.6) as well as the more diffuse densities. This was reasonable since the non-idempotent matrix representation could fit the modified structure factor data more closely, due to the larger number of parameters and

FIGURE III

Comparison of unconstrained densities, with and without temperature compensation in the basis functions. $c_1 = 0.8$, $\xi_f = 0.95$

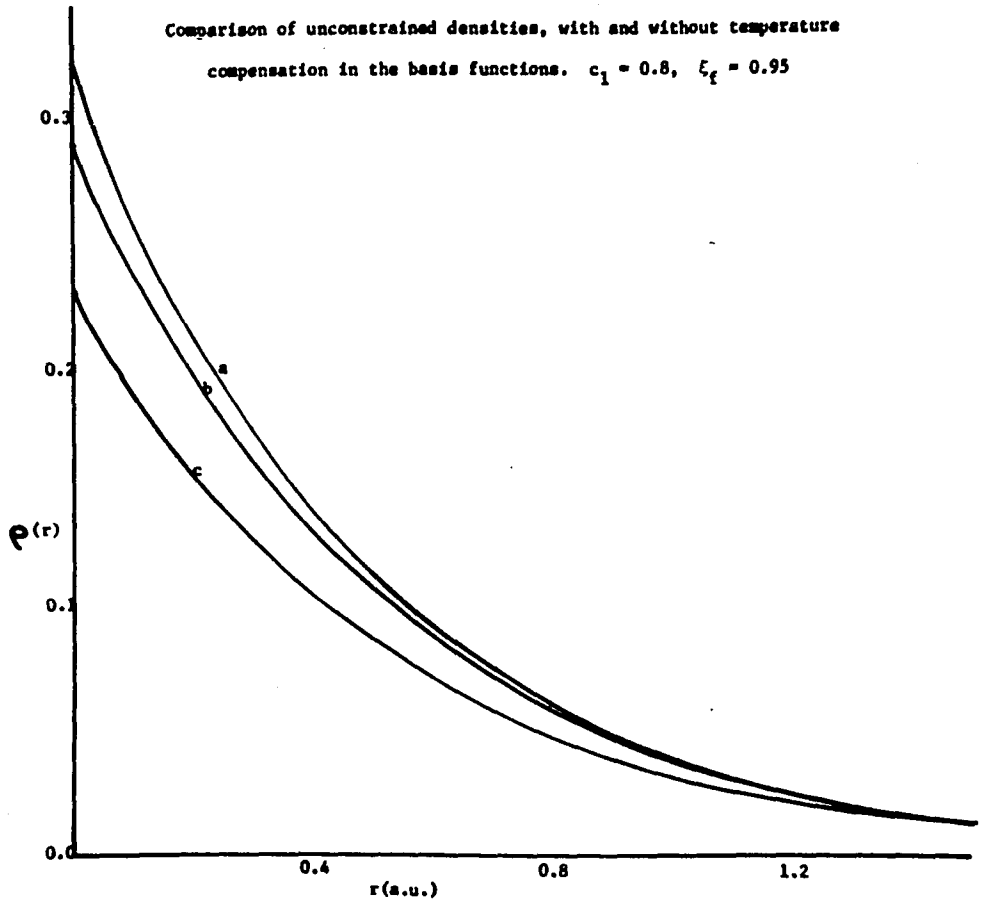

a) Model static density

b) Density obtained when $\psi_i \rightarrow \psi_i e^{-\alpha \sin^2\theta/\lambda^2}$

c) Density obtained when ψ_i is unmodified

FIGURE IV

Comparison of idempotent densities with and without temperature compensation in the basis functions $c_1 = 0.8$, $\xi_f = 0.95$

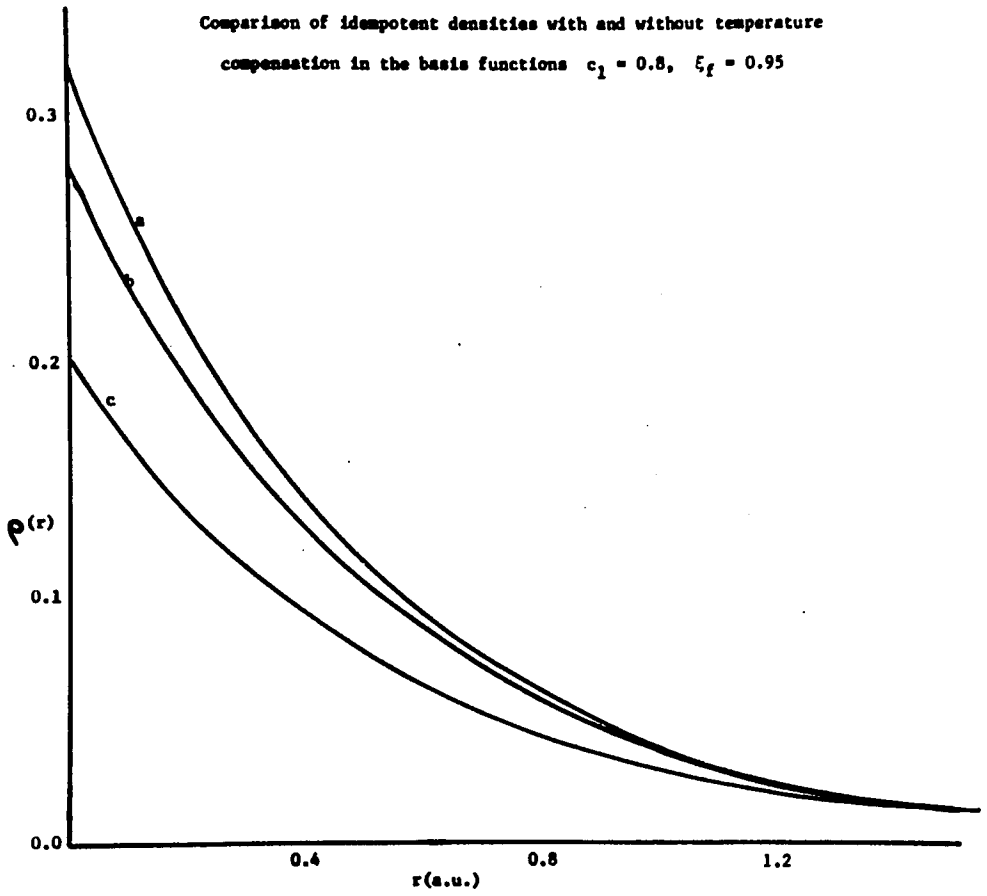

a) Model static density

b) Density obtained when $\psi_i \rightarrow \psi_i e^{-\alpha \sin^2\theta/\lambda^2}$

c) Density obtained when ψ_i is unmodified

TABLE XVII

Comparison of Energy Expectation Values for $\underset{\sim}{P}_N$ and $\underset{\sim}{P}_I$.

	-<E>					
	$\underset{\sim}{P}_N$			$\underset{\sim}{P}_I$		
ξ_f	a)	b)	c)	a)	b)	c)
.98	.3651	.4112	.3667	.3739	.4656	.3731
.99	.3650	.4126	.3658	.3695	.4651	.3691
1.0	.3650	.4142	.3650	.3650	.4646	.3650
1.01	.3650	.4158	.3642	.3604	.4641	.3608
1.02	.3650	.4636	.3634	.3556	.4636	.3565

$c_1 = 0.8$

In all calculations $0 \quad \sin\theta/\lambda \quad 0.8$, 0.02 $\mathring{A}^{-1}$

a) F(K) from a static model density. Basis functions are 1s and 2s hydrogenic (δ_f)

b) $F(K)e^{-4 \sin^2\theta/\lambda^2}$ Basis functions as in a)

c) $F(K)e^{-4 \sin^2\theta/\lambda^2}$ Basis functions $1se^{-2 \sin^2\theta/\lambda^2}$ and $2se^{-2 \sin^2\theta/\lambda^2}$.

The difference between columns a) and c) is due to weighting factors $\omega_K = 1.0$ and $\omega_K = e^{-2 \sin^2\theta/\lambda^2}$ respectively, in the functionals

$$\mathcal{F} = \sum_K \omega_K \left[\mathrm{Tr}\, \underset{\sim}{P}\xi(k) - F(k) \right]^2$$

The value of the correct <E> is given with $\xi = 1.0$ in columns a) and c).

thus reflected a thermally smeared density, which was smaller than the static model density at small values of r. This is illustrated in Figure V. In this study in the one case of $c_1 = 0.8$, an idempotent density resulted from the best fit to $Fe^{-B\sin^2\theta/\lambda^2}$ which was more diffuse than the non-idempotent density. It can be seen from Table XVIII that this was the one case in which the elements of $\underset{\sim}{P}_N$ were closer to the elements of the model $\underset{\sim}{P}$ than were those of $\underset{\sim}{P}_I$.

In comparing the matrix elements P_{ij} with those obtained when no modification of either F(K) or the basis functions was considered, an interesting observation was made. It appeared that the corresponding elements of the $\underset{\sim}{P}_I$ matrix did not differ as much as those of the P_N matrix. This is shown in Table XIX. In Table XX it is seen that this was reflected in the expectation value $\langle 1/r \rangle$ to a somewhat smaller extent. This offered a possible explanation for the results obtained in Chapter IV in which $\underset{\sim}{P}_I$ was seen to predict a better value of $\langle 1/r \rangle$ as the model density became more diffuse. In general, the greatest contribution to the functional from

$$\Delta = \mathrm{Tr}\, \underset{\sim}{P}\, \underset{\sim}{f}(k) - F(k)$$

was in regions of K space where the structure factor was large. As the density became more diffuse this region was contracted more and more into the low scattering angle region. Thus, in a sense, attempting to fit to more diffuse model densities is analagous to emphasizing the low scattering angle data. The smaller difference in the elements of $\underset{\sim}{P}_I$ when the

FIGURE V

Comparison of densities obtained when the Debye Waller Factor is introduced into the structure factor $c_1 = 0.6$, $\xi_f = 1.0$

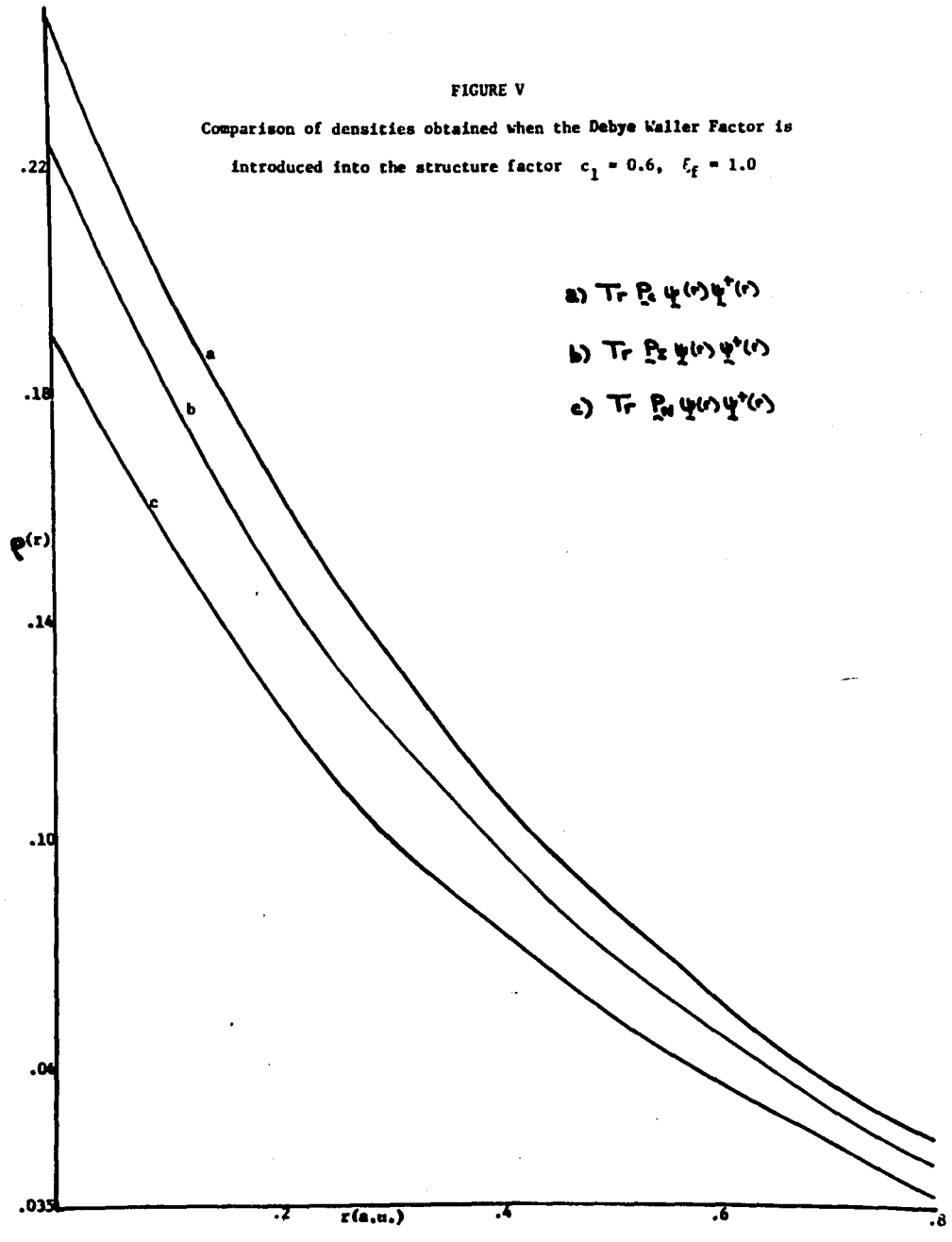

TABLE XVIII

$\underset{\sim}{P}$ matrix elements when the Debye Waller factor is introduced into the structure factor.

$P_c(1,1)$	$P_c(1,2)$	$P_c(2,2)$	$P_N(1,1)$	$P_N(1,2)$	$P_N(2,2)$	$P_I(1,1)$	$P_I(1,2)$	$P_I(2,2)$
1.000	0.000	0.000	1.116	-.4745	-.116	.9672	-.1780	.032
.6400	.4800	.3600	.7711	-.0169	.2286	.9057	-.2923	.094
.3600	.4800	.6400	.4628	-.1015	.5372	.2962	.4566	.703
.1600	.3666	.8400	.2304	.1141	.7696	.1253	.3311	.874
.0400	.1960	.9600	.0801	.0563	.9199	.0269	.1617	.973

$F(K) = F_o(K)e^{-4 \sin^2\theta/\lambda^2}$

Basis functions are hydrogenic 1s and 2s with no temperature factor, and $\xi_f = 1.0$.

TABLE XIX

Comparison of the elements of the $\underset{\sim}{P}$ matrices with different weighting factors.

c_1	$\Delta P_I(1,1)$	$\Delta P_I(1,2)$	$\Delta P_N(1,1)$	$\Delta P_N(1,2)$
.8	.0062	.0014	.0107	.0285
.6	.0032	.0001	.0119	.0315
.4	.0010	.0010	.0119	.0313
.2	.0002	.0005	.0110	.0291

ΔP_{ij} is the difference between P_{ij} elements obtained by minimizing

$$\mathcal{F} = \sum_k \left[\mathrm{Tr}\, P \underset{\sim}{f}(k) - F(k) \right]^2$$

and minimizing

$$\mathcal{F} = \sum_k e^{-2\sin^2\theta/\lambda^2} \left[\mathrm{Tr}\, \underset{\sim}{P}\, \underset{\sim}{f}(k) - F(k) \right]^2$$

Note that $\Delta P(1,1) = \Delta P(2,2)$.

TABLE XX

Comparison of $\langle 1/r \rangle$ obtained from P_N and P_I with different weighting factors.

	$\underset{\sim}{P}_N$		$\underset{\sim}{P}_I$		$\underset{\sim}{P}_c$
C_1	a)	b)	a)	b)	
.8	.9175	.9136	.9049	.9016	.9311
.6	.7079	.7038	.7040	.7015	.7211
.4	.5117	.5079	.5126	.5116	.5236
.2	.3521	.3487	.3552	.3556	.3621

$\underset{\sim}{P}_N$ and $\underset{\sim}{P}_I$ are representations in the hydrogenic basis set with $\xi_f = 0.95$

$\underset{\sim}{P}_c$ is the model representation in the hydrogenic basis set with $\xi = 1.0$.

a) $\langle 1/r \rangle$ obtained from $\underset{\sim}{P}_N$ or $\underset{\sim}{P}_I$ minimized with $w_K = 1.0$

b) $\langle 1/r \rangle$ obtained from P_N or P_I minimized with $w_K = e^{-2 \sin^2\theta/\lambda^2}$.

c_1	$\Delta\langle 1/r \rangle_{PN}$	$\Delta\langle 1/r \rangle_{PI}$
.8	.0039	.0033
.6	.0041	.0025
.4	.0048	.0010
.2	.0034	.0004

$\Delta\langle 1/r \rangle$ is the difference between $\langle 1/r \rangle$ obtained with $w_K = 1.0$ and $w_K = e^{-2 \sin^2\theta/\lambda^2}$.

different weighting factors were used implied that a preferential fit to the low scattering angle data, to some extent constrained the fit to the total K space for $\underset{\sim}{P}_I$. This was less true for $\underset{\sim}{P}_N$, where the closer fit to lower scattering angles occurred at the expense of the fit to the higher scattering angles. This was reflected in a good fit to the model densities at larger values of r at the expense of the fit close to the nucleus.

The results discussed in the present chapter indicated that if the structure factor obtained from a thermally smeared density is accurately represented by $F_o(K)\, e^{-B\sin^2\theta/\lambda^2}$, the corresponding static density could be obtained by modifying each basis function i.e. $\psi_i \rightarrow \psi_i e^{-B/2\sin^2\theta/\lambda^2}$. It also appeared that the idempotent matrix representation was less sensitive to different weighting schemes in this method.

Chapter VI

Reference was made in Chapter I to calculation of the matrix representative of the one electron density for the molecule tetracyanoethylene oxide (TCEO) by Matthews et al[21]. The method used[20] was briefly described in Chapter I, the main feature of interest here being that the matrix representative of the density was not constrained to be N-Representable. This being the case it was of interest to calculate the eigenvalues λ, of the one electron densities described by the authors, in order to determine whether the fell in the quantum mechanically valid range

$$o \leq \lambda \leq 2.0 \quad [29] \qquad \text{(see Chapter II)}$$

The published $\underset{\sim}{P}$ matrices were obtained using Hartree-Fock and Slater-Type Orbital basis functions. Both the one and two center approximations were used with the STO basis set and it is the three $\underset{\sim}{P}$ matrices obtained with this basis set which have been analyzed here. The two $\underset{\sim}{P}$ matrices obtained from the one center approximation differed in the number of symmetry constraints which were imposed, in order to reduce the number of parameters.

It was noted in Chapter II that diagonalization of the matrix representative $\underset{\sim}{P}$, of the one electron density in an orthonormal basis set gives rise to the eigenvalues of the density which appear as the diagonal elements of the diagonal matrix $\underset{\sim}{\bar{P}}$. Dr. Matthews collaborated with us in this study, sending us the complete overlap matrix in the STO basis set in the inertial frame of reference (see FigureVI) and the

transformation matrices required to convert the basis vectors in the cartesian coordinate system, centered on each atom and between bonds (see Figure VI) into the inertial coordinate basis vectors. i.e. the transformation matrices $\underset{\sim}{T}$ perform the following rotations

$$\underset{\sim}{\Psi}(\text{atom}) = \underset{\sim}{T}(\text{atom})\ \underset{\sim}{\Psi}(\text{inertial})$$

$$\underset{\sim}{\Psi}(\text{bond}) = T(\text{bond})\ \underset{\sim}{\Psi}(\text{inertial})$$

Henceforth subscripts a, b, and i will denote matrices referring to the cartesian coordinate basis vectors centered on atoms and between bonds and to the basis vectors in the inertial frame of reference, respectively. $\underset{\sim}{T}_a$ and $\underset{\sim}{T}_b$ will be used to denote the transformation matrices described above. The published $\underset{\sim}{P}$ matrices obtained from the one center approximation were representations of the density in the Cartesian coordinate basis vectors centered on each atom. It was thus necessary to transfrom these matrices into representations of the density in an orthonormal basis set and then to diagonalize the transformed matrices. This was accomplished as follows: -

Since $$\underset{\sim}{\Psi}_a \cdot \underset{\sim}{\Psi}_a^{+} = \underset{\sim}{S}_a$$

and $$\underset{\sim}{\Psi}_a = \underset{\sim}{T}_a\ \underset{\sim}{\Psi}_i$$

then $$\underset{\sim}{S}_a = \underset{\sim}{T}_a\ \underset{\sim}{\Psi}_i \cdot \underset{\sim}{\Psi}_i^{+} \underset{\sim}{T}_a^{+}$$

$$= \underset{\sim}{T}_a\ \underset{\sim}{S}_i\ \underset{\sim}{T}_a^{+}$$

Then since $$\underset{\sim}{S}_a^{-1/2}\ \underset{\sim}{\Psi}_a = \underset{\sim}{\Psi}'_a$$

where $\underset{\sim}{\Psi}'_a$ are orthonormal due to

$$\underset{\sim}{\Psi}'_a \cdot \underset{\sim}{\Psi}'^{+}_a = \underset{\sim}{S}_a^{-1/2} \underset{\sim}{\Psi}_a \cdot \underset{\sim}{\Psi}_a^{+} \underset{\sim}{S}_a^{-1/2} = \underset{\sim}{S}_a^{-1/2} \underset{\sim}{S}_a \underset{\sim}{S}_a^{-1/2} = \underset{\sim}{1}$$

the one electron density may be written

$$\begin{aligned} \rho(\vec{r}) &= \mathrm{Tr}\, \underset{\sim}{P}_a \underset{\sim}{\Psi}_a \underset{\sim}{\Psi}_a^{+} \\ &= \mathrm{Tr}\, \underset{\sim}{P}_a \underset{\sim}{S}_a^{1/2} \underset{\sim}{S}_a^{-1/2} \underset{\sim}{\Psi}_a \underset{\sim}{\Psi}_a^{+} \underset{\sim}{S}_a^{-1/2} \underset{\sim}{S}_a^{1/2} \\ &= \mathrm{Tr}\, \underset{\sim}{S}_a^{1/2} \underset{\sim}{P}_a \underset{\sim}{S}_a^{1/2} \underset{\sim}{\Psi}'_a \underset{\sim}{\Psi}'^{+}_a \end{aligned}$$

The overlap matrix in the intertial system was transformed to the atomic coordinate system and the matrix

$$\underset{\sim}{S}_a^{1/2} \underset{\sim}{P}_a \underset{\sim}{S}_a^{1/2}$$

was diagonalized.

It should be noted that diagonalization of the matrix representation of the density in the inertial basis set should give the same results. Thus, as a check on the results the diagonalization was repeated, using the following transformations

$$\begin{aligned} \rho(\vec{r}) &= \mathrm{Tr}\, \underset{\sim}{P}_a \underset{\sim}{\Psi}_a \underset{\sim}{\Psi}_a^{+} \\ &= \mathrm{Tr}\, \underset{\sim}{P}_a (\underset{\sim}{T}_a \underset{\sim}{\Psi}_i)(\underset{\sim}{\Psi}_i^{+} \underset{\sim}{T}_a^{+}) \\ &= \mathrm{Tr}\, \underset{\sim}{T}_a^{+} \underset{\sim}{P}_a \underset{\sim}{T}_a \underset{\sim}{\Psi}_i \underset{\sim}{\Psi}_i^{+} \\ &= \mathrm{Tr}\, \underset{\sim}{P}_i \underset{\sim}{\Psi}_i \underset{\sim}{\Psi}_i^{+} \\ &= \mathrm{Tr}\, \underset{\sim}{P}_i \underset{\sim}{S}_i^{1/2} \underset{\sim}{S}_i^{-1/2} \underset{\sim}{\Psi}_i \underset{\sim}{\Psi}_i^{+} \underset{\sim}{S}_i^{-1/2} \underset{\sim}{S}_i^{1/2} \\ &= \mathrm{Tr}\, \underset{\sim}{S}_i^{1/2} \underset{\sim}{P}_i \underset{\sim}{S}_i^{1/2} \underset{\sim}{\Psi}'_i \underset{\sim}{\Psi}'^{+}_i \end{aligned}$$

The matrix $\underset{\sim}{P}_I$ was obtained from the published matrix $\underset{\sim}{P}_a$, as above, and the matrix

$$\underset{\sim}{S}_i^{1/2}\,\underset{\sim}{P}_i\,\underset{\sim}{S}_i^{1/2}$$

was diagonalized. The eigenvalues obtained from both diagonalizations were identical.

In the two center approximation the off diagonal terms in the published $\underset{\sim}{P}$ matrix referred to cartesian coordiante basis vectors oriented in directions, referred to as the bond directions (see Figure VI). The matrix to be diagonalized in this case was obtained through the following transformations.

$$\rho(\vec{r}) = \sum_n \mathrm{Tr}\, \underset{\sim}{P}_{an}\, \underset{\sim}{\psi}_{an}\, \underset{\sim}{\psi}_{an} + 2 \sum_{n<m} \mathrm{Tr}\, \underset{\sim}{P}_{nm}\, \underset{\sim}{\psi}_{mb}\, \underset{\sim}{\psi}_{nb}$$

where $\underset{\sim}{P}_{an}$ is the block diagonal in the total $\underset{\sim}{P}$ matrix corresponding to atom n. $\underset{\sim}{\psi}_{an}$ are the basis functions in the cartesian coordinate system (Figure **VI**) centered on atom n.

$\underset{\sim}{P}_{nm}$ is an off diagonal block in the total $\underset{\sim}{P}$ matrix corresponding to bonded atoms n and m.

$\underset{\sim}{\psi}_{nb}$ and $\underset{\sim}{\psi}_{mb}$ are basis functions for atoms n and m oriented in the bond direction, shown between the atoms in Figure **VI**.

Thus
$$\rho(\vec{r}) = \sum_n \mathrm{Tr}\, \underset{\sim}{P}_{an}\, \underset{\sim}{T}_{an}\, \underset{\sim}{\psi}_{in}\, \underset{\sim}{\psi}_{in}^{+}\, \underset{\sim}{T}_{an}^{+} + 2 \sum_{n<m} \mathrm{Tr}\, \underset{\sim}{P}_{nm}\, \underset{\sim}{T}_{bnm}\, \underset{\sim}{\psi}_{im} \underset{\sim}{\psi}_{in}^{+}\, \underset{\sim}{T}_{bnm}^{+}$$

where the transformation matrices $\underset{\sim}{T}_a$ and $\underset{\sim}{T}_b$ are those for each atom and bond.

$\rho(\vec{r})$ thus reduces to

$$\rho(\vec{r}) = \sum_n \mathrm{Tr}\, \underset{\sim}{T}_{an}^{+}\, \underset{\sim}{P}_{an}\, \underset{\sim}{T}_{an}\, \underset{\sim}{\psi}_{in}\, \underset{\sim}{\psi}_{in}^{+} + 2 \sum_{n<m} \mathrm{Tr}\, \underset{\sim}{T}_{bnm}^{+}\, \underset{\sim}{P}_{nm}\, \underset{\sim}{T}_{bnm}\, \underset{\sim}{\psi}_{im}\, \underset{\sim}{\psi}_{in}^{+}$$

This defines the transformations which must be applied the occupied blocks of the published $\underset{\sim}{P}$ matrix, in order to convert it into a matrix representation of the density in the inertial basis set. However the inertial basis set was normalized but not orthogonal so a final transformation was required viz.

$$\underset{\sim}{S}_i^{1/2}\ \underset{\sim}{P}_i\ \underset{\sim}{S}_i^{1/2}$$

where $\underset{\sim}{P}_i$ contains the diagonal blocks $\underset{\sim}{T}_{an}^{+}\ \underset{\sim}{P}_{an}\ \underset{\sim}{T}_{an}$

and the off diagonal blocks corresponding to bonded atoms

$$\underset{\sim}{T}_{bnm}^{+}\ \underset{\sim}{P}_{nm}\ \underset{\sim}{T}_{bnm}$$

In order to ensure that the correct transformations were indeed being carried out the trace of each block in $\underset{\sim}{P}_i$ was compared with the total atom and bond populations given by Matthews et al[21]. (i.e. those given in Table IV, reference 21). The numbers agreed and thus the normalization of the $\underset{\sim}{P}$ matrix was maintained. The matrix $\underset{\sim}{S}^{1/2}\ \underset{\sim}{P}_i\ \underset{\sim}{S}^{1/2}$ was diagonalized. After all diagonalization procedures the diagonal matrix was routinely transformed back into the original matrix via

$$\underset{\sim}{U}\ \underset{\sim}{\bar{P}}\ \underset{\sim}{U}^{+} = \underset{\sim}{P}$$

to ensure that the diagonalization procedure was correct.

The results are shown in Tables XX, XXI, XXII Seven of the eigenvalues of each one electron density obtained from the one center approximation, fell outside the quantum mechancially valid range. The eigenvalues greater than 2.0 are however quite similar, showing as expected that the non N-Representability of the one electron density is not specifi-

cally dependent on the number or type of symmetry restrictions used in this method, but rather, is due to the fundamental neglect of constraints which explicity ensure N-Representability. Twenty-six of the eigenvalues of the one electron density obtained from the two center approximation fell outside the quantum mechanically valid range. The results were surpriseing in that large positive and negative eigenvalues were obtained. However Carol Frishberg[8], has found that large negative eigenvalues may be obtained when the idempotency constraint is neglected in the fit of hydrogenic 1s, 2s and 3s basis functions to the best spherical hydrogen atom density of Stewart et al[30]. Analysis of my own results, discussed in Chapters III-V shows that large positive or negative values of the independent parameter $P_N(1,2)$ result in the quantum mechanically invalid negative densities and the violation of the variational principle. In the calculation of the one electron density of TCEO, fifty-five basis functions were used. In this case the meaning of a "large off-diagonal element" in the $\underset{\sim}{P}$ matrix is not clear. However since the magnitude of the eigenvalues obtained by Carol Frishberg using the three hydrogenic basis functions was larger than those obtained in a similar study (see Chapter II) using only two hydrogenic basis functions it is possible that the larger number of independent off diagonal elements is responsible for the larger eigenvalues. It is noted that fewer eigenvalues fall outside the quantum mechanically valid range and those which do are smaller in magnitude, for the density obtained from the one center approximation. In this calcula-

tion all off diagonal elements in the $\underset{\sim}{P}$ matrix which correspond to basis functions on different atoms are set to 0.

TABLE XXI

Eigenvalues of the one electron density, from the One Center Approximation, of TCEO.

0.19	1.01	2.00
0.20	1.02	2.00
0.20	1.11	2.00
0.21	1.18	2.00
0.24	1.21	2.00
0.26	1.23	2.00
0.28	1.26	2.00
0.32	1.29	2.00
0.36	1.31	2.00
0.39	1.33	2.03
0.42	1.41	2.07
0.44	1.46	2.54
0.51	1.51	2.59
0.53	1.53	2.62
0.56	1.58	2.69
0.58	1.67	2.96
0.62	1.74	
0.66	1.93	
0.72	2.00	

The matrix representation of the density is displayed in Table II reference 21.

TABLE XXII

Eigenvalues of the one electron density, from the One Center Approximation, of TCEO.

0.18	0.97	2.00
0.19	1.04	2.00
0.19	1.13	2.00
0.20	1.16	2.00
0.22	1.20	2.00
0.24	1.22	2.00
0.27	1.25	2.00
0.29	1.27	2.00
0.33	1.28	2.00
0.34	1.36	2.00
0.38	1.39	2.05
0.40	1.47	2.11
0.47	1.52	2.58
0.53	1.53	2.65
0.56	1.58	2.71
0.60	1.66	2.74
0.63	1.84	3.02
0.67	1.93	
0.72	2.00	

The matrix representation of the density is displayed in Table III reference 21.

TABLE XXIII

Eigenvalues of the one electron density, from the Two Center Approximation, of TCEO.

-13.37	0.30	2.00	6.45
- 5.92	0.34	2.00	8.42
- 3.64	0.40	2.00	15.42
- 2.93	0.43	2.03	
		2.14	
- 2.61	0.49	2.19	
- 1.95	1.83	2.31	
- 1.44	1.90	2.36	
- 1.21	1.95	2.37	
- 0.92	1.99	2.44	
0.07	2.00	2.44	
0.07	2.00	2.49	
0.09	2.00	2.56	
0.24	2.00	2.66	
0.24	2.00	2.76	
0.25	2.00	3.72	
0.25	2.00	4.34	
0.26	2.00	5.74	

The matrix representation of the density is displayed in Table IV reference 21.

FIGURE VI

Inertial Frame of Reference

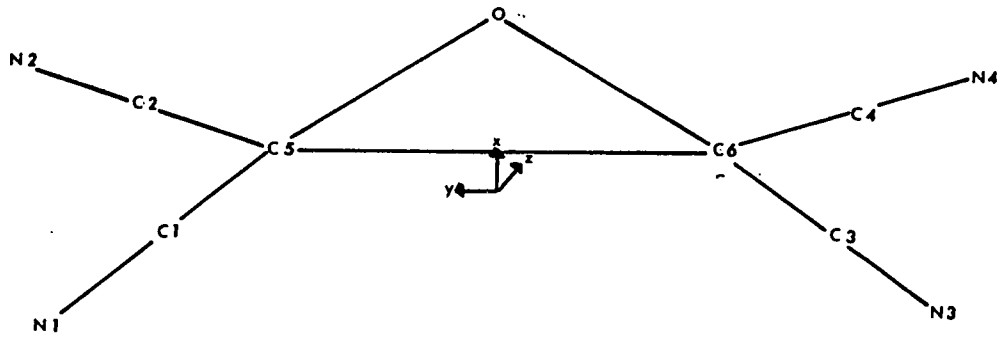

$\hat{x}$ and $\hat{y}$ are approximately in the C_5 - O - C_6 plane

$\hat{z}$ is out of the plane of the paper

Atom and Bond Cartesian Coordinate System

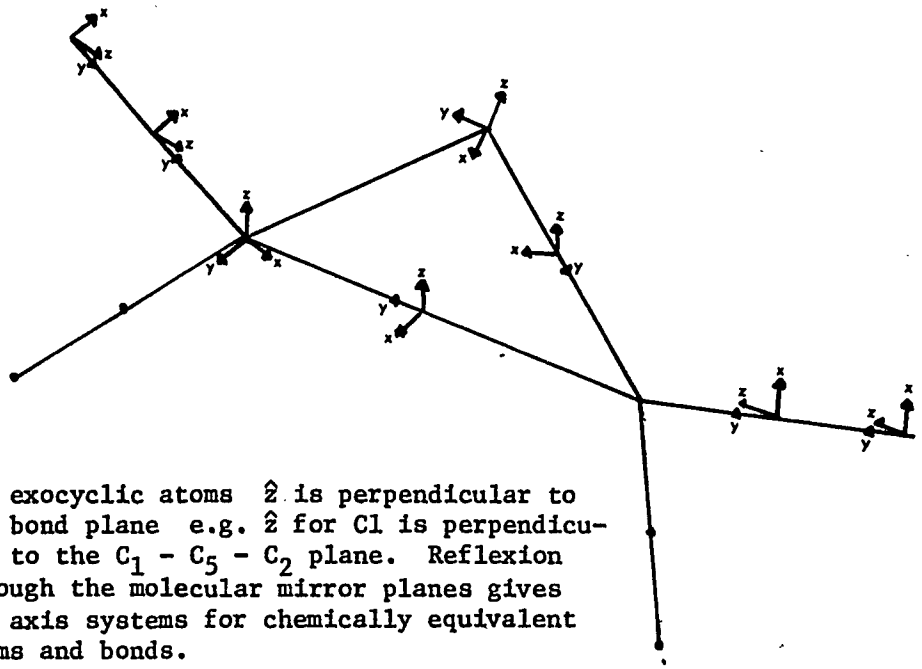

For exocyclic atoms $\hat{z}$ is perpendicular to the bond plane e.g. $\hat{z}$ for Cl is perpendicular to the C_1 - C_5 - C_2 plane. Reflexion through the molecular mirror planes gives the axis systems for chemically equivalent atoms and bonds.

Appendix I

The fourier transforms of the 1s and 2s hydrogenic orbitals are as follows

$$f_{11} = \int 1s\,1s\, e^{2\pi i \vec{k}.\vec{r}}\, d^3\vec{r} = \xi^3/\pi\, I_0(2\xi, G)$$

$$f_{12} = \int 1s\,2s\, e^{2\pi i \vec{k}.\vec{r}}\, d^3r = \xi^3/\pi \frac{1}{\sqrt{8}} \left\{ I_0(3/2\,\xi, G) - \xi/2\, I_1(3/2\,\xi, G) \right.$$

$$f_{22} = \int 2s\,2s\, e^{2\pi i \vec{k}.\vec{r}}\, d^3r = \xi^3/8\pi \left\{ I_0(\xi, G) - \xi I_1(\xi, G) + \frac{\xi^2}{4} I_2(\xi, G) \right\}$$

$$I_0(\alpha, G) = 8\pi\alpha \,/\, (\alpha^2 + G^2)^2$$

$$I_1(\alpha, G) = 8\pi\,(3\alpha^2 - G^2) \,/\, (\alpha^2 + G^2)^3$$

$$I_2(\alpha, G) = 96\pi\,(\alpha^3 - \alpha G^2) \,/\, (\alpha^2 + G^2)^4$$

$G = 4\pi a_0 \sin\theta/\lambda$ a.u.$^{-1}$

where $\sin\theta/\lambda$ is in $A^{\circ -1}$

and $a_0 = 0.5291772\ \text{Å}/\text{a.u.}$

Appendix II

The least squares equations for $\underset{\sim}{P}_N$ were calculated as follows: -

$$\underset{\sim}{P}_N = \begin{pmatrix} 1-p & q \\ q & p \end{pmatrix} \qquad \underset{\sim}{f}(K) = \begin{pmatrix} f_{11}(K) & f_{12}(K) \\ f_{21}(K) & f_{22}(K) \end{pmatrix}$$

where $f_{12}(K) = f_{21}(K)$

Thus $\mathrm{Tr}\ \underset{\sim}{P}_N\ \underset{\sim}{f}(K)$

$$= (1-p)\ f_{11}(K) + 2q\ f_{12}(K) + p\ f_{22}(K)$$

$$= f_{11}(K) + (f_{22}(K) - f_{11}(K))\ p + 2q\ f_{12}(K)$$

To minimize

$$F = \sum_K \omega_K \left[\mathrm{Tr}\ \underset{\sim}{P}_N\ \underset{\sim}{f}(k) - F(k) \right]^2$$

calculate

$$\partial F/\partial p = \sum_K \omega_K\, 2 \left[\mathrm{Tr}\ \underset{\sim}{P}_N\ \underset{\sim}{f}(k) - F(k) \right] \left(f_{22}(k) - f_{11}(k) \right) = 0$$

$$\partial F/\partial q = \sum_K \omega_K\, 2 \left[\mathrm{Tr}\ \underset{\sim}{P}_N\ \underset{\sim}{f}(k) - F(k) \right] \left(2 f_{12}(k) \right) = 0$$

i.e. $$\sum_K 2\omega_K \left\{ \left(f_{22}(k) - f_{11}(k) \right)^2 p + 2q\, f_{12}(k) \left(f_{22}(k) - f_{11}(k) \right) \right\}$$

$$= \sum_K 2\omega_K \left\{ F(k) \left(f_{22}(k) - f_{11}(k) \right) - f_{11}(k) \left(f_{22}(k) - f_{11}(k) \right) \right\}$$

and $$\sum_K 2\omega_K \left\{ 4q\, f_{12}(k)^2 + \left(f_{22}(k) - f_{11}(k) \right) 2 f_{12}(k)\, p \right\}$$

$$= \sum_K 2\omega_K \left\{ F(k)\, 2 f_{12}(k) - 2 f_{11}(k)\, f_{12}(k) \right\}$$

In matrix notation

$$\underset{\sim}{B}\ \underset{\sim}{A} = \underset{\sim}{C}$$

where $\underset{\sim}{A} = \begin{pmatrix} p \\ q \end{pmatrix}$

thus $b_{11} = \sum_k 2\omega_k \left(f_{22}(k) - f_{11}(k)\right)^2$

$b_{12} = \sum_k 4\omega_k f_{12}(k) \left(f_{22}(k) - f_{11}(k)\right)$

$b_{21} = \sum_k 4\omega_k f_{12}(k) \left(f_{22}(k) - f_{11}(k)\right)$

$b_{22} = \sum_k 8\omega_k f_{12}(k)^2$

$c_1 = \sum_k 2\omega_k \left\{ F(k) \left(f_{22}(k) - f_{11}(k)\right) - f_{11}(k)\left(f_{22}(k) - f_{11}(k)\right)\right\}$

$c_2 = \sum_k 4\omega_k \left\{ F(k) f_{12}(k) - f_{11}(k) f_{12}(k)\right\}$

To obtain p and q

$$\underset{\sim}{A} = \underset{\sim}{B}^{-1} \underset{\sim}{C}$$

The least squares equations for $\underset{\sim}{P}_I$ were calculated as follows: -

$$\underset{\sim}{P}_I = \begin{pmatrix} (1-p) & \pm p^{1/2}(1-p)^{1/2} \\ \pm p^{1/2}(1-p)^{1/2} & p \end{pmatrix}$$

We require to minimize

$$H = \sum_k \omega_k \left[\mathrm{Tr}\, \underset{\sim}{P}\underset{\sim}{f}(k) - F(k)\right]^2$$

$$= \sum_k \omega_k \left[\left(\mathrm{Tr}\, \underset{\sim}{P}\underset{\sim}{f}(k)\right)^2 + F^2(k) - 2F(k)\,\mathrm{Tr}\, \underset{\sim}{P}\underset{\sim}{f}(k)\right]$$

with respect to p. Inserting $\underset{\sim}{P}_I$ into the above equation reduces it to: -

$$H = ap^2 + bp + c \pm p^{1/2}(1-p)^{1/2} d \pm p p^{1/2}(1-p)^{1/2} e$$

where

$$a = \sum_k w_k \left\{ f_{11}(k)^2 + f_{22}(k)^2 - 2 f_{11}(k) f_{22}(k) + 4 f_{12}(k)^2 \right\}$$

$$b = \sum_k w_k \left\{ 2F(k) f_{11}(k) - 2F(k) f_{22}(k) - 2 f_{11}(k)^2 + 4 f_{12}(k)^2 + 2 f_{11}(k) f_{22}(k) \right\}$$

$$c = \sum_k w_k \left\{ f_{11}(k)^2 - 2F(k) f_{11}(k) + F(k)^2 \right\}$$

$$d = \sum_k w_k \left\{ 4 f_{11}(k) f_{12}(k) - 4 F(k) f_{12}(k) \right\}$$

$$e = \sum_k w_k \left\{ 4 f_{12}(k) f_{22}(k) - 4 f_{11}(k) f_{12}(k) \right\}$$

Thus

$$\partial F/\partial p = 2ap + b \pm d\left[(1-2p)/2p^{1/2}(1-p)^{1/2}\right] \pm e\left[(3p-4p^2)/2p^{1/2}(1-p)^{1/2}\right] = 0$$

i.e.

$$2ap + b = \mp \frac{1}{p^{1/2}(1-p)^{1/2}} \frac{1}{2} \left\{ d(1-2p) + e(3p-4p^2) \right\}$$

squaring both sides

$$p(1-p)(2ap+b)^2 = \frac{1}{4} \left\{ d - 2pd + 3pe - 4p^2 e \right\}^2$$

reduces the expression to

$$p^4 c_5 + p^3 c_4 + p^2 c_3 + p c_2 + c_1 = 0$$

where

$$c_5 = 4e^2 + 4a^2$$

$$c_4 = 4ab - 4a^2 - 2e(3e-2d)$$

$$c_3 = b^2 - 4ab - 2ed + \tfrac{1}{4}(3e-2d)^2$$

$$c_2 = \tfrac{1}{2}d(3e-2d) - b^2$$

$$c_1 = \tfrac{1}{4}d^2$$

The solution of the fourth order equation in the range $0 \leq p \leq 1$ which gives the smallest value of $\overline{\text{FF}}$ is the required solution.

Appendix III

During the course of this work, calculations were undertaken as an extension of the study of Clinton and Massa.[24] Certain numerical errors were discovered and the tables reproduced on the following pages are the corrected tables to be compared with those previously published. It should be noted that the results in the corrected tables in no way alter the conclusions previously drawn by the authors.

TABLE XXIV

Eigenvalues (N_1 and N_2) of $\underset{\sim}{P}_{NI}$ and $\underset{\sim}{P}_I$ for various values of orbital exponent ξ.

	$\underset{\sim}{P}_{NI}$		P_I	
ξ	N_1	N_2	N_1	N_2
.98	1.315	-0.315	1.	0.
1.00	1.226	-0.226	1.	0.
1.02	1.149	-0.149	1.	0.
1.04	1.086	-0.086	1.	0.

To be compared with Table III Phys. Rev. Lett. 29, 1363 (1972).

TABLE XXV

Elements of the density matrix for systematic errors in the scattering factor data via $F \rightarrow sF$, $1.00 \leqslant S \leqslant 1.04$. The orbital exponent is in all cases $\xi = 1.0$.

S	$P_{NI}(1s,1s)$	$P_{NI}(1s,2s)$	$P_{NI}(2s,2s)$	$P_{I}(1s,1s)$	$P_{I}(1s,2s)$	$P_{I}(2s,2s)$
1.00	.8006	.6610	.1994	.9039	.2947	.0961
1.02	.8168	.6765	.1832	.9070	.2905	.0930
1.04	.8330	.6919	.1670	.9092	.2873	.0908

To be compared with Table IV Phys. Rev. Lett. 29, 1363 (1972).

TABLE XXVI

Elements of the density matrix for changes in the scattering factor data via $F \rightarrow F \exp(-BG^2)$.

B	$P_{NI}(1s,1s)$	$P_{NI}(1s,2s)$	$P_{NI}(2s,2s)$	$P_I(1s,1s)$	$P_I(1s,2s)$	$P_I(2s,2s)$
0	.8006	.6610	.1994	.9039	.2947	.0961
0.2	.8355	.5734	.1645	.9060	.2918	.0940
0.4	.8681	.4911	.1319	.9087	.2881	.0913

To be compared with Table V Phys. Rev. Lett. 29, 1363 (1972).

TABLE XXVII

Elements of the density matrix for changes in the scattering factor data via $F \rightarrow F \exp(-BG^2)$ and for corresponding changes in the basis $\Psi \rightarrow \Psi \exp(-BG^2/_2)$. The orbital exponent is $\xi = 1.0$.

B	$P_{NI}(1s,1s)$	$P_{NI}(1s,2s)$	$P_{NI}(2s,2s)$	$P_I(1s,1s)$	$P_I(1s,2s)$	$P_I(2s,2s)$
0	.8006	.6610	.1994	.9039	.2947	.0961
0.2	.8048	.6520	.1952	.9048	.2935	.0952
0.4	.8098	.6433	.1910	.9057	.2923	.0943

To be compared with Table VI Phys. Rev. Lett. 29, 1363 (1972).

Bibliography

1. for e.g. Matthews and Stucky
J. Am. Chem. Soc. 93:23 5945 (1971).

2. Coppens Science 153, 1577, (1967).

3. Halgren, Anderson, Jones and Lipscomb
Phys. Lett. 8, 547, (1971).

4. Becker, Coppens and Ross
J. Am. Chem. Soc. 95, 7604, (1973).

5. Coppens Acta Cryst. B30 255 (1974).

6. Coppens, Pautler and Griffin
J. Am. Chem. Soc. 93 1051 (1971)

7. O'Connell Acta Cryst. B24 1273 (1969).

8. Carol Frishberg, Thesis: "Idempotent Matrices and X-Ray Diffraction Data" (1975).

9. Coppens "Measurement of Electron Densities in Solids by X-Ray Diffraction" Preprint 1974.

10. Coppens Acta Cryst. B27 1931 (1971).

11. Dunitz Acta Cryst. B29 589 (1973).

12. Coppens Trans. Am. Cryst. Soc. 93 (1972).

13. Stewart J. Chem. Phys. 48 4882 (1968).

14. e.g. Dawson Proc. Roy. Soc. A298, 264 (1967).

15. Stewart J. Chem. Phys. 53 205 (1970).

16. McWeeney Acta Cryst. 6, 631 (1953)

17. Stewart J. Chem. Phys. 51 4569 (1969).

18. Stewart J. Chem. Phys. 52 431 (1970).

19. Stewart J. Chem. Phys. 50 2485, (1969).

20. Coppens, Willoughby and Csonka Acta. A27, 248 (1971).

21. Matthews, Stucky and Coppens J. Am. Chem. Soc. 94:23, 8001 (1970)

22. Jones, Pautler and Coppens Acta Cryst. A28, 635 (1972).

23. Clinton and Massa Trans. Am. Cryst. Ass. 149 (1972).

24. Clinton and Massa Phys. Rev. Lett. 29, 1363 (1972).

25. Clinton, Frishberg, Massa and Oldfield Int. Journal of Quantum Chemistry 7, 505 (1973).

26. Stewart J. Chem. Phys. 57 1664 (1972).

27. McWeeney Rev. Mod. Phys. 32 335 (1960).

28. Clinton, Galli and Massa Phys. Rev. 177, 1 (1969).

29. Lowdin Phys. Rev. 97 1474, (1955).

30. Stewart, Davidson and Simpson J. Chem. Phys. 42, 3175 (1965).